Repetitive Firing: A Quantitative Study of Feedback in Model Encoders

J. F. FOHLMEISTER, R. E. POPPELE, and R. L. PURPLE

From the Laboratory of Neurophysiology, University of Minnesota, Minneapolis, Minnesota 55455

ABSTRACT   Recognition of nonlinearities in the neuronal encoding of repetitive spike trains has generated a number of models to explain this behavior. Here we develop the mathematics and a set of tests for two such models: the leaky integrator and the variable-γ model. Both of these are nearly sufficient to explain the dynamic behavior of a number of repetitively firing, sensory neurons. Model parameters can be related to possible underlying basic mechanisms. Summed and nonsummed, spike-locked negative feedback are examined in conjunction with the models. Transfer functions are formulated to predict responses to steady state, steps, and sinusoidally varying stimuli in which output data are the times of spike-train events only. An electrical analog model for the leaky integrator is tested to verify predicted responses. Curve fitting and parameter variation techniques are explored for the purpose of extracting basic model parameters from spike train data. Sinusoidal analysis of spike trains appear to be a very accurate method for determining spike-locked feedback parameters, and it is to a large extent a model independent method that may also be applied to neuronal responses.

INTRODUCTION

These papers are part of a series presented over the past several years in which we have attempted to develop a quantitative model that is sufficient to explain the observed repetitive firing behavior of certain sensory neurons (Purple and Salasin, 1969; Poppele, 1970b; Purple, 1970; Rescigno et al., 1970; Poppele and Purple, 1971; Poppele and Chen, 1972; Fohlmeister, 1973; Fohlmeister et al., 1974a, b, c, 1975). The aim has been to find a mathematical model capable of completely describing observed behavior, particularly the dynamic behavior, and that can also serve as a basis for understanding underlying mechanisms. In addition, we have sought the simplest model (i.e. the one with the least number of parameters) that is consistent with this aim.

The approach has been to employ methods of system identification that are based on spike train analysis. The advantages of the analysis are that it is relatively noninvasive, allowing the system to operate normally, and that it gives information about events occurring at the trigger zone where repetitive firing is taking place. Much emphasis is placed on the use of cyclic stimuli which are a natural means of exciting a system whose parameters vary periodically. Interactions between the periodicities in encoder parameters and stimulus produce patterns of output pulses that contain information about the dynamic properties of encoder parameters (Rescigno et al., 1970; Fohlmeister et al., 1974a).

Repetitive firing may be defined as the occurrence of a train of action potentials in response to a constant current stimulus. Many sensory neurons are capable of firing repetitively at very low rates, a property not shared in general by the axon. It implies that some process, not described by Hodgkin-Huxley types of models for the action potential, delays the occurrence of a spike to prolong sufficiently the interspike interval. The search for a model adequate to describe this behavior began when Adrian (1928) showed how a time-varying threshold after a spike could account for a prolongation of the interspike interval. Indeed many models involving threshold and/or membrane impedance changes will qualitatively account for slow repetitive firing (e.g., Kernell, 1968; Kernell and Sjöholm, 1972, 1973; Katz, 1939; Michaelis and Chaplain, 1973). However, few of these models have been extensively tested quantitatively or under dynamic conditions.

The study of encoder dynamics has been largely in terms of simplified models, beginning with the analysis of the integrate-and-fire model of Knight (1969). Although the steady-state input-output characteristics of this model are linear, as is often the case for sensory neurons, its response to cyclic inputs was shown to be quite different. By simply introducing a leak to the integrator, however, the dynamics of the model response become similar to those observed for sensory neurons (Stein and French, 1970; Poppele, 1970a; Knight, 1972). These dynamics have been described for the response to sinusoidal inputs in terms of Bode plots of gain and phase and they result from an entrainment interaction occurring between the pacemaker rhythm of the encoder and the frequency of the sinusoidal stimulus (Rescigno et al., 1970). The model parameter γ [the relaxation rate, which is equal to $(RC)^{-1}$ of a leaky integrator analog] is uniquely defined by the Bode plot and the rate of firing of the unmodulated encoder (f_0).

It was then shown that the "γ" of sensory neurons is not a constant, as in the model, but is a variable which depends on the duration of the interspike interval, in such a manner that

$$\gamma \propto f_0,$$

(Poppele and Chen, 1972). Furthermore, it was shown that there were at least two ways of determining the model γ from pulse train analysis and the application of these two techniques to sensory neurons gives two different values. These experimental findings were reconciled with a third model, which is a further generalization of the two described above.

In this model γ is a state variable that depends on time and membrane voltage (Fohlmeister, 1973). The variable-γ model accounted both for the experimental observations outlined above, and for the observed ratio $\bar{\gamma}/\gamma_e \doteq 2$ where $\bar{\gamma}$ and γ_e are the values of γ obtained by the two measurement techniques (Fohlmeister et al., 1974a). In addition, the model makes at least two predictions that are supported by independent observations: (a) that membrane loading (corresponding to γ in the model) is large at the beginning of the interspike interval after the spike, and then becomes small; and (b) that this parameter can be reset by hyperpolarization.

Even though the correspondence between the variable-γ model and sensory neuron behavior is very close, there are certain systematic discrepancies particularly for those neurons known to contain mechanisms that introduce spike-

locked feedback to the encoding process. The interaction of pacemaker activity and feedback has been explored previously for the linear integrator model both by mathematical analysis (Knight, 1969) and analog simulation (Purple and Salasin, 1969) and it was shown that the qualitative effect is a decrease in low frequency gain whose time constant and magnitude depend on the parameters of the feedback (see also Barbi et al., 1975, who consider feedback for the leaky integrator model). Since this corresponded qualitatively to a discrepancy observed between model and neuron we have proceeded, generally and quantitatively, to explore the effects of encoder feedback.

In this paper, we present a mathematical analysis of two kinds of spike-locked feedback in the context of the leaky integrator model. With this model the problem can be treated mathematically in closed form and the results of that analysis also account quantitatively for the dynamic behavior of the variable-γ model with feedback (which can be analyzed only by numerical integration). In addition, we compare the results of the mathematical analysis with the dynamic behavior of an electrical analog of the leaky integrator. This allows us to determine directly from Bode plot data the magnitude of the parameters used in the analog. Thus, it is proposed that spike train analysis can be used not only to determine the presence of encoder feedback, but also to determine the magnitude and time course of that feedback.

MATERIALS AND METHODS

Experiments were conducted on an electrical analog of the "leaky integrator" encoder (French and Stein, 1970). The essential functional elements consist of an RC impedance which integrates an applied current to produce an output voltage. As the voltage reaches a threshold level, a pulse is produced and the integrator is reset. Two types of feedback were incorporated into the analog: summed and nonsummed feedback. In both cases an output pulse is inverted, shaped by a low pass filter, and added to the input current. In the case of nonsummed feedback the signal resets the integrator to a given minimum value while the summed feedback always changes the integrator value by a given amount. The basic difference is that summed feedback can accumulate from one interval to the next while nonsummed feedback cannot.

The analog device is driven by a current source that can be modulated to produce step changes in current or sinusoidally modulated current at various modulation frequencies. Output pulses are timed, along with synchronization pulses from the current modulator by an on-line computer (IBM 1800 Data Acquisition and Control System, IBM Corp., White Plains, N. Y.).

One object of the experiments is to provide a check on the mathematical analysis of the model which is based on a linearization of pulse train parameters using first order perturbation theory (Knight, 1969). In this context, the problem we face with the experimental data is to extract the modulation component from among the many carrier and side-band components present in the spectrum of a frequency-modulated pulse train. The problem has been discussed in previous work and there are, in fact, many ways to solve it (e.g., Matthews and Stein, 1969; Knox, 1970; Poppele and Bowman, 1970; Knight, 1972). One basic method is filtering, to isolate the modulation frequency. A second is averaging, to suppress carrier and side-band components that have a random phase with respect to the modulation (Bayly, 1968). The simplest application of these two processes is the cycle histogram technique of estimating the probability density of impulse occurrence in a single cycle of modulation. Filtering is accomplished in this method by histogram binning; frequency components with periods shorter than two bin widths are

filtered out as are frequency components lower than the single cycle chosen for the averaging base. There are two problems in using this technique. One is that it requires a large data sample. If we use harmonic distortion as an index of how well the modulation component is isolated, then we find that this measure depends on the length of the sample and on the depth of modulation (Knox, 1970). For small modulations of a regular pulse train $(f_1/f_0 \lesssim 0.1$, see glossary below), about 10,000 events must be averaged before a distortion of the order of 5% can be expected when five harmonics are computed. This is about a 10-fold improvement over what can be expected with a noisy pulse train (Knox, 1970), but it is still a rather large data sample. When larger modulation depths are used, the convergence is faster only if the pulse train is generated by a linear integrator (Knight, 1969). If the leaky integrator is used, there is a phase-locking between modulation and carrier components so that these latter components can no longer be suppressed by averaging (Rescigno et al., 1970; see also Fig. 1). The analysis technique we use can overcome both of these problems.[1]

We use a binning technique similar to the cycle histogram, however, instead of merely adding a count to a bin when a pulse occurs, the interval since the last pulse is measured and that value is saved in a particular bin. The average interval for each bin is then calculated and its reciprocal, the average "instantaneous frequency" is plotted as the value for each bin (see Poppele and Bowman, 1970). Because frequency is determined by an exact measure of interval length, it takes very few data points to give the desired answer. Thus, with 100–200 pulses we can determine the modulation component with near zero harmonic distortion. For large modulations, however, where there is a large difference between maximum and minimum intervals, a phase distortion is introduced because of the nonlinear relation between interval and frequency. In the example shown in Fig. 1, where the modulation (f_1/f_0) was about 0.35, the distortion due to this effect was about 6%, with resulting error in phase determination of the order of 1–2°. The technique has also another disadvantage in that it is extremely sensitive to noise. One extra pulse added to an otherwise smoothly modulated train can induce a large error in the estimate of the modulation component. This is because that extra pulse can produce an extra-short interval, represented in the reciprocal by a very high instantaneous frequency, thereby distorting the average for some bin. If one used the histogram technique that extra pulse would have the same weighting factor as all the other pulses in a particular bin and it would therefore not greatly disturb the value for that bin.

Both of these problems (phase distortion and noise sensitivity) can be avoided by using relatively low modulation depths (<0.3) and by selecting data to avoid noise. In that domain the technique has the advantages of rapid analysis with short data samples and a relative insensitivity to phase locking (Fig. 1). The latter property results because the technique depends on filtering rather than averaging. The parameters of the filter are determined by the interspike interval so that frequency components with periods shorter than two interspike intervals are suppressed. Thus components occurring at the carrier frequency, such as those illustrated in Fig. 1, are removed by filtering. This is equivalent to choosing a bin width for the cycle histogram that is equal to the interspike interval. If that technique were used we would introduce another problem for modulation frequencies close to the pulse repetition rate of the pulse train, since there would be very few bins,

---

[1] It can be pointed out here that the most direct solution to this problem is to apply a Fourier analysis directly to the pulse train. In general, this requires that all data points be saved, which can require a large memory capacity and therefore become costly. With the histogram or binning techniques, it is only necessary to provide storage to accommodate the number of bins used since the binning can be done in real time. In addition the Fourier analysis based on equally spaced points over a cycle (e.g., Karmen and Boit, 1940) is in general faster than most Fourier analysis algorithms. Therefore, with the binning and the fast Fourier transform the entire analysis can be conveniently accomplished on line.

although a certain minimum number of bins is required in order accurately to fit the modulation. We have found that at least 11 binned points are needed in the determination of Fourier components to give the most accurate results. With five points, for example, there is a systematic underestimation of amplitude of the order of 6%. Little if any improvement in accuracy is achieved if more than 11 points are used. Therefore, with the exception of the analysis plotted in Fig. 1, all analyses in these papers were made from 11-point determinations of the first 12 sine and cosine coefficients of the Fourier series
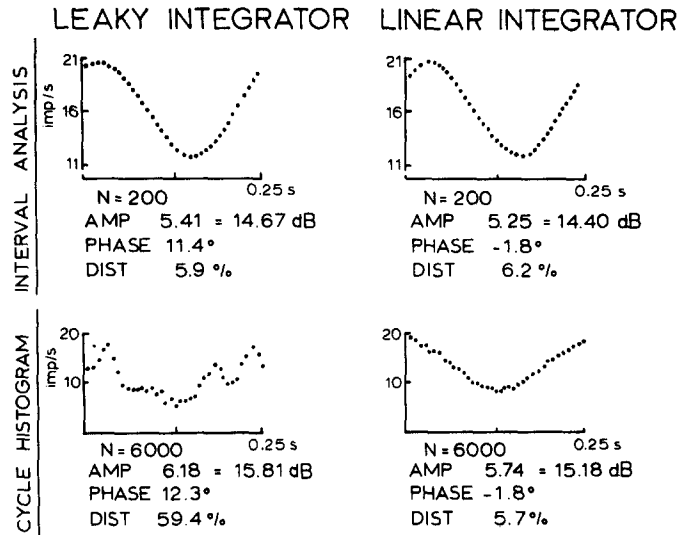
LEAKY INTEGRATOR   LINEAR INTEGRATOR

INTERVAL ANALYSIS

imp/s

N = 200   0.25 s
AMP   5.41 = 14.67 dB
PHASE 11.4°
DIST   5.9 %

N = 200   0.25 s
AMP   5.25 = 14.40 dB
PHASE -1.8°
DIST   6.2 %

CYCLE HISTOGRAM

imp/s

N = 6000   0.25 s
AMP   6.18 = 15.81 dB
PHASE 12.3°
DIST   59.4 %

N = 6000   0.25 s
AMP   5.74 = 15.18 dB
PHASE -1.8°
DIST   5.7%

FIGURE 1. Methods of spike train analysis. Two model encoders, the linear integrator and the leaky integrator (RC = 37 ms) were driven at 16 pulses/s and modulated at 4 Hz to ±5.3 pulses/s. Pulse train data were analyzed by cycle histogram binning (below) and average interval binning (above). 37 bins were used in each case. The interval plots have not been normalized for the zero-order hold (see McKean et al., 1970) but calculations of amplitude and phase have been. For the interval binning, 200 pulses were used in the analysis and the distortion did not improve with larger samples. In order to obtain the same value of distortion with cycle histogram analysis for the linear integrator, 6,000 pulses were required. With the leaky integrator, the cycle histogram shows peaks corresponding to phase-locked carrier components which could not be suppressed by averaging. Even so, the Fourier analysis of this histogram gives accurate values of amplitude and phase. The theoretical phase for the leaky integrator at this modulation frequency is 12.6° and for the linear integrator it is 0°.

that best fits the 11 binned data points. The fundamental component is reported as amplitude ($|f_1|$, imp/s) or as gain, defined here as:

$$20 \log_{10} \frac{|f_1|}{K},$$

and its phase with respect to the applied modulation is ϕ.[2] The first five harmonics are

[2] In general we plot either a normalized gain for the purpose of matching the shapes of gain curves or else we plot only the output, expressed in *db*. Thus *K* has the dimensions of imp/s and its value is 1 in the latter case, because the input is treated as an unknown for the purpose of curve fitting experimental data to theory. It is done this way because the input in the theoretical equations is proportional to, but not the same as the input used in the experiment, and we do not, in general, know the proportionality constant.

used to determine the harmonic distortion, which is the root mean square amplitude of these components as a percent of the amplitude of the fundamental. Results of the analysis are plotted as Bode plots in which gain and phase are plotted as functions of the logarithm of the modulation frequency, ω.

Computations of leaky integrator behavior were made on the IBM 1800 directly from equations presented in the results. The variable-γ model presented in Results is defined by the following pair of coupled equations:

$$\dot{u} = -\gamma u + s,$$
$$\dot{\gamma} = -B\gamma + Du,$$

(Fohlmeister, 1973) supplemented with a specific initial condition for γ at the beginning of each interspike interval (symbols defined below). Calculations of its behavior were computed by numerical integration with the Continuous Systems Modeling Program of IBM for the 1800. For details see Fohlmeister, 1973, and Fohlmeister et al., 1974a.

The symbols used for various functions and variables are largely drawn from previous work (Knight, 1972; Fohlmeister, 1973) and are given here in a glossary for convenient reference.

Symbols	Units	Meaning
A	volts	threshold
B	seconds^{-1}	rate constant in variable-γ model
C	farad	integrator capacitance (leaky integrator, also total cell capacitance)
D	seconds^{-2}-volt^{-1}	constant in variable-γ model
f_0	impulse/second	mean rate of output pulses
f_1	impulse/second	change in rate about f_0 of a sinusoidally modulated pulse train
f_m	Hertz,	modulation frequency
g	mho	encoder membrane conductance
h	volt/second	magnitude of drive reduction introduced by summed feedback
H	volt/second	instantaneous value of summed feedback
i_0	ampere	mean level of input current
i_1	ampere	amplitude of sinusoidal current
k	volt/second	magnitude of drive reduction by nonsummed feedback
R	ohm	integrator resistance
s_0	volt/second	mean level of drive
s_1	volt/second	amplitude of sinusoidal drive
T_0	second	interspike interval in the absence of modulation
T_1	second	perturbation of interspike interval due to modulation
u	volt	voltage across RC integrator also membrane voltage
γ	second^{-1}	integrator rate constant—also state variable in variable-γ
ϕ	radians or degrees	phase angle between input and output
ϕ'	radians	arbitrary phase of input
τ	second	time constant of summed feedback
τ_f	second	time constant of frequency decay following step stimulus
τ_k	second	time constant of nonsummed feedback
ω	radian/second	modulation frequency

Definitions

$s = i/C$

$\gamma = 1/RC$ (leaky integrator model)

$\gamma = g/C$ (variable-γ model)

$\omega = 2\pi f_m$

RESULTS

The results are presented in five parts. The first develops the leaky integrator as a mathematical model which is the basis of the electrical analog whose properties are described in parts II and III. Part IV deals with the sensitivity of the analysis technique as a means of determining model parameters. In the final part we compare the results of the analysis with the behavior of a more realistic model for neuronal repetitive firing — the variable-γ model.

I. *The Model*

The leaky integrator has been considered as a model for a neuronal encoder and some of its properties have been presented in recent publications (Stein and French, 1970; Knight, 1972; Poppele and Chen, 1972; Fohlmeister et al., 1974a). In this section, we will extend those descriptions to include nonsummed and summed feedback (see Materials and Methods) and present a mathematical description of the steady state, transient, and modulated behavior of this device (see also Barbi et al., 1975).

   STEADY STATE   Steady-state operation of the encoder is defined as that due to a constant drive (denoted by s_0) which evokes a train of pulses with constant interval T_0. This behavior is expected both in the absence and in the presence of feedback (asymptotically in the case of summed feedback). Ignoring feedback for the moment, however, we will consider an encoder subject to drive s_0 that produces a pulse when the time integral of the drive reaches a threshold voltage A. Because of the non-zero encoder conductance, there are losses associated with the integration process such that the drive at time $\hat{t}$ is effectively diminished at the later time of integration t' to the amount $s_0 \cdot \exp[-(t' - \hat{t}')\gamma]$. To arrive at this particular form, the magnitude of the loss is assumed to be proportional to the potential u generated by the drive, and the leak parameter γ is introduced as the proportionality constant (Fohlmeister et al., 1974a). This leads to the characteristic exponential charging curve of the constant $RC(= 1/\gamma)$ circuit whose voltage time course under constant drive $s_0 = i_0/C$ is given by the equation

$$i_0 = \frac{1}{R} \cdot u + C \frac{du}{dt} \quad \text{or} \quad s_0 = \gamma u + \dot{u}, \dot{u} \equiv \frac{du}{dt}. \tag{I.1}$$

This equation integrates — between the limits $u = 0$ (at $t = 0$) and $u = A$ (at $t = T_0$) — to:

$$A = \int_0^{T_0} s_0 e^{-(T_0 - t)\gamma} \, dt. \tag{I.2}$$

The integral leads to the following steady-state relation among A, T_0, and s_0:

$$A = \frac{s_0}{\gamma}(1 - e^{-T_0\gamma}). \tag{I.3}$$

In the limit of the nonleaky integrator, $\gamma \to 0$, this relation reduces to:

$$A = s_0 T_0.$$

(Knight, 1969, 1972). For purposes of this paper, threshold is assumed constant (see Discussion).

FEEDBACK   Inhibitory feedback is defined for the present as any effect which satisfies these two conditions: that the effect is initiated by an action potential occuring in a cell; and that the effect subtracts from the stimulus to that cell. An electrogenic sodium pump in the slowly adapting stretch receptor of the crayfish, and self-inhibition in the *Limulus* eccentric cell are the mechanisms for feedback that are studied experimentally in the companion paper (Fohlmeister et al., 1977). The feedback sums from impulse to impulse and declines almost exponentially with time (Stevens, 1964; Solokove and Cooke, 1971).

In addition to summed feedback we treat here also a possible channel of nonsummed feedback that could be a mechanism for producing an afterpotential for the leaky integrator which resembles that of the sensory neurons. For this channel we denote the initial reduction in stimulus after an impulse by the symbol k and its relaxation time constant by τ_k. The drive following each pulse then becomes

$$s_0 - k\, e^{-t/\tau_k}, \tag{I.4}$$

a function of time and of the time of occurrence of pulses. Any remaining component of the effective reduction in drive at the end of an interpulse interval is eradicated by the following pulse which again reduces the initial value of the drive by the amount k to follow Eq. (I.4) in the subsequent interval. Therefore such feedback will not contribute to adaptation after the second pulse.

Summed feedback, in contrast, adds any remaining component of its feedback at the end of an interpulse interval to the pulse-initiated amount h, which decays with a time constant τ. For the case of summed feedback, the term to be added to s_0 asymptotically takes the form:

$$s_0 \to s_0 - h\left(\sum_{m=0}^{\infty} e^{-mT_0/\tau}\right) e^{-t/\tau} \equiv s_0 - H(t). \tag{I.5}$$

The infinite series is the summed residual effect of the feedback from an infinite number of previous pulses.

The steady-state integral with both types of feedback becomes:

$$A = \int_0^{T_0} [s_0 - k\, e^{-t/\tau_k} - h\left(\sum_{m=0}^{\infty} e^{-mT_0/\tau}\right) e^{-t/\tau}] e^{-(T_0 - t)\gamma}\, dt. \tag{I.6}$$

So long as the interpulse period T_0 is constant, the geometric series in the summed term adds to $(1 - e^{-T_0/\tau})^{-1}$ and Eq. (I.6) integrates to

$$A = \frac{s_0}{\gamma}(1 - e^{-T_0\gamma}) - \frac{h}{\gamma - \dfrac{1}{\tau}}\cdot\frac{e^{-T_0/\tau} - e^{-t_0\gamma}}{1 - e^{-T_0/\tau}} - \frac{k}{\gamma - \dfrac{1}{\tau_k}}(e^{-T_0/\tau_k} - e^{-T_0\gamma}). \tag{I.7}$$

In the limit of the nonleaky integrator ($\gamma = 0$) and summed feedback only, this reduces to the result of Knight (1969):

$$A = s_0 T_0 - h\tau. \tag{I.8}$$

TRANSIENT BEHAVIOR   The two types of feedback have different effects on the transient behavior of the encoder, such as that exhibited when a step change in driving current is applied. Since the effect of nonsummed feedback is not carried over from interval to interval, all intervals are identical for any given s_0. Summed feedback, on the other hand, will induce adaptive behavior due to the accumulation of feedback. Succeeding intervals will be identical only when the amount of feedback added by a pulse equals that removed by the end of each interval.

As will be described later[3] the accumulated feedback $H(t)$ in response to a step change in drive to s_0 may be considered a differentiable function of time, provided that $H(t)$ is defined as the average of the instantaneous amount of feedback over the interval at time t. Thus $H(t)$, which has the dimensions of h (and therefore of the stimulus s_0), will enter the charging equation of the leaky integrator as

$$\dot{u} = -\gamma u + s_0 - H(t). \tag{I.9}$$

Anticipating results to be presented separately (see footnote 3) we are led to the following relation between steady-state frequency and mean feedback:

$$H(\infty) = h\tau f(\infty), \tag{I.10}$$

where the terms $H(\infty)$ and $f(\infty)$ refer to the instantaneous summed feedback and the instantaneous frequency at long times (steady state) after a step. Further, if the frequency decay to $f(\infty)$ is exponential with the time constant τ_f (which is the case for the leaky integrator, cf. Part III, analog-transient behavior):

$$f(t) = [f(0) - f(\infty)] \exp (-t/\tau_f) + f(\infty), \tag{I.11}$$

then there results the following relation among τ_f, τ, and h:

$$\tau_f = \left[1 + \frac{\tau h A [f(\infty)]^2}{[s_0 - H(\infty) - \gamma A][s_0 - H(\infty)]} \right]^{-1} \cdot \tau. \tag{I.12}$$

Thus, for the leaky integrator τ_f is a function of s_0 for a given τ and h and further $\tau_f < \tau$ always.

From the transient response to a step stimulus one may further derive an expression for h as a function of an early interspike interval length T_l after the step. If τ is much greater than the sum of the first few intervals, the summed feedback will not have decayed substantially by the time of the interval T_l. Under these conditions Eq. (I.6) with summed feedback only specializes to

$$A \doteq \int_0^{T_l} dt[s_0 - lh] \exp (t - T_l)\gamma,$$

[3] J. F. Fohlmeister. Manuscript in preparation.

which integrates to

$$A \doteq \frac{s_0 - lh}{\gamma}(1 - e^{-T_l \cdot \gamma}).$$ (I.13)

Rearranging leads to

$$h = \frac{1}{l}\left[\frac{A\gamma}{\exp(-T_l \cdot \gamma) - 1} + s_0\right],$$ (I.14)

where l is the (small) integer of the number of the interval after the change in drive from zero to s_0. Further, if γ is small such that $T_l \cdot \gamma \to 0$, Eq. (I.14) becomes

$$h \doteq \frac{1}{l}\left[s_0 - \frac{A}{T_l}\right],$$ (I.15)

under this special condition. In both cases (I.14 and I.15), different magnitudes of h for a given τ will result in different rates of adaptation.

SINUSOIDAL MODULATION   With the steady-state problem solved in closed form in Eq. (I.7) we now turn to the more general case where the steady-state drive is perturbed by a sinusoid of angular frequency ω:

$$s(t) = s_0 + s_1 e^{j\omega t}.$$ (I.16)

A perturbation technique is employed to derive the transfer function. The derivation, as well as definition of the notation which has appeared previously (Barbi et al., 1975), is relegated to the Appendix.[4] The transfer function with one channel each of summed and nonsummed feedback is given by

$$\frac{f_1}{s_1} = \frac{f_0}{s_0} \cdot \frac{j\omega}{j\omega + \gamma} \cdot \frac{1 - e^{(j\omega + \gamma)/f_0}}{1 - e^{j\omega/f_0}}\left[M + \frac{K}{e^{j\omega/f_0} - e^{-1/\tau f_0}}\right]^{-1},$$ (I.17)

where M and K are real and dimensionless, and have the form

$$M \equiv 1 + \frac{h}{s_0} \cdot \frac{e^{(\gamma - \frac{1}{\tau})/f_0} - \tau\gamma}{(\tau\gamma - 1)(1 - e^{-1/\tau f_0})} + \frac{k}{s_0} \cdot \frac{e^{(\gamma - \frac{1}{\tau_k})/f_0} - \tau_k\gamma}{\tau_k\gamma - 1},$$ (I.18)

$$K \equiv \frac{h}{s_0}\left(\frac{1}{e^{1/\tau f_0} - 1}\right)\frac{e^{(\gamma - \frac{1}{\tau})/f_0} - 1}{\tau\gamma - 1}.$$ (I.19)

The amplitude is given by

$$\left|\frac{f_1}{s_1}\right| = \frac{f_0}{s_0}\frac{\omega}{\sqrt{\omega^2 + \gamma^2}}\left[\frac{F(\gamma/f_0)}{F(0)}\right]^{1/2}$$ (I.20)

$$\left[\frac{F(-1/\tau f_0)}{K^2 + M^2 F(-1/\tau f_0) + 2MK(\cos\omega/f_0 - e^{-1/\tau f_0})}\right]^{1/2}$$

[4] Our derivation differs chiefly by the introduction into the. equations of multiple channels of feedback, either summed or nonsummed, or both.

where

$$F(x) \equiv e^{2x} + 1 - 2e^x \cos \omega/f_0. \qquad (I.21)$$

All feedback dependence in Eq. (I.20) is contained in the final factor.[5] In the absence of summed feedback $K = 0$, the final factor reduces to M^{-1}. Thus nonsummed feedback alone does not alter the ω dependence of the gain curve for the leaky integrator with a given γ although it does result in an overall shift. In the absence of all feedback $K = 0$, $M = 1$; the final factor reduces to unity leading to the no-feedback gain curve

$$\left|\frac{f_1}{s_1}\right| = \frac{f_0}{s_0} \cdot \frac{\omega}{\sqrt{\omega^2 + \gamma^2}} \left[\frac{F(\gamma/f_0)}{F(0)}\right]^{1/2},$$

(Fohlmeister et al., 1974a, Eq. [1.1]).

Since F is symmetric about $\omega = \pi f_0$, summed feedback contributes a factor to the gain curve which is symmetric about a value halfway between $\omega = 0$ and ω equal to the steady-state firing (angular) frequency $2\pi f_0$. In addition for positive h, τ, and γ, the feedback factor always enhances the gain in the middle ($\omega = \pi f_0$) relative to the ends ($\omega = 0, 2\pi f_0$). The infinity in the gain curve at $\omega = 2\pi f_0$ however, continues to dominate the finite values of the feedback factor as depicted in the figures. The $\omega = 0$ limit of the gain curve is

$$\left|\frac{f_1}{s_1}\right|_{\omega \to 0} \to \frac{f_0}{s_0} \cdot \frac{f_0}{\gamma} (e^{\gamma/f_0} - 1) \cdot \frac{1 - e^{-1/\tau f_0}}{K + M(1 - e^{-1/\tau f_0})}. \qquad (I.22)$$

The phase curve, defined as

$$\text{phase} = \text{Arctan} \frac{Im(f_1/s_1)}{Re(f_1/s_1)}, \qquad (I.23)$$

is given by

$$\text{phase} = \text{Arctan} \frac{\gamma \cdot ReN + \omega \cdot ImN}{\omega \cdot ReN - \gamma \cdot ImN}, \qquad (I.24)$$

where

$$ReN = ReU \cdot ReV - ImU \cdot ImV, \qquad (I.25a)$$

$$ImN = ReU \cdot ImV + ImU \cdot ReV, \qquad (I.25b)$$

and where in turn

$$ReU = 1/2(1 - e^{\gamma/f_0})F(0), \qquad (I.26a)$$

$$ImU = (1 - e^{\gamma/f_0}) \sin \omega/f_0, \qquad (I.26b)$$

$$ReV = M + K[\cos \omega/f_0 - \exp(-1/\tau f_0)]/F(-1/\tau f_0), \qquad (I.26c)$$

$$ImV = K \sin (\omega/f_0)/F(-1/\tau f_0). \qquad (I.26d)$$

[5] $F(x)$, unlike M and K, is strongly dependent upon omega. Hence Eq. (I.20) is not strictly formatted to separate the dependence on driving frequency from the dependence on fixed parameters, but instead only separates feedback effects for algebraic convenience.

The variables M and K are those of Eq. (I.18) and (I.19). An important consequence of this phase curve is that in the absence of summed feedback $K = 0$, the phase is identical to the no-feedback case (Eq. (I.2) of Fohlmeister et al., 1974 a). That is to say that nonsummed feedback alone has no effect on the phase. This is an important point for resolving an ambiguity about the origin of afterpotentials in repetitive spike trains (see part V below).

II. Electrical Analog Behavior without Feedback

In the following sections the behavior of the model, as expressed in Eq. (I.3) and (I.17) is compared with the behavior of an electrical analog. The analog is a particular member of the general class described by the model where the loss in the integrator is due to an RC impedance such that:

$$\gamma = \frac{1}{RC} \, . \qquad (II.1)$$

STEADY-STATE BEHAVIOR The steady-state behavior of these encoders is defined by the relation between steady-state drive (s_0) and the resulting rate of output pulses (f_0). From Eq. (I.3):

$$f_0 = -\gamma/ln\left(1 - \frac{A\gamma}{s_0}\right), \qquad (II.2)$$

where A is the threshold voltage (Knight, 1972, Eq. [5.5]). Therefore, the effect of the drive on the pulse rate depends only on the leak so long as the threshold is constant. Furthermore, there is a minimum effective drive:

$$s_{min} = \gamma A, \qquad (II.3)$$

since smaller drives do not overcome the leak and the voltage fails to reach threshold. The relation expressed in Eq. (II.2) is nonlinear, but it can be seen from Fig. 2 (solid lines), which is a plot of Eq. (II.2) for five different values of γ, that f_0 increases nearly linearly with s_0 over a range of values. This has special significance for the results which will be presented below with sinusoidal modulations. In deriving the dynamic relation between drive and pulse rate, it is assumed that the drive is given a small perturbation about a particular steady-state operating point. In general, the analysis works well for input excursions which remain within a small neighborhood of the operating point, but of itself the analysis has little predictive value for excursions which carry the solution away from that neighborhood. However, the results presented below indicate that even responses to relatively large excursions are accurately predicted by the derived function (for an explanation of this, see Modulated Behavior, below, and Knight, 1972).

Actually, however, there is no completely linear relation between f_0 and drive except in the limit where $\gamma \to 0$. In this case:

$$\lim_{\gamma \to 0} s_0 = f_0 A, \qquad (II.4)$$

which is also the asymptotic relation between f_0 and drive for the leaky encoder as $s_0 \to \infty$. Therefore, the change in f_0 for a given change in s_0 is always greater

for the leaky case than for the nonleaky case; moreover, the greater the leak, the steeper this slope (see Fig. 2). It follows then that for low modulation frequencies ($<f_0/4$) the absolute gain of the leaky encoder is likewise greater for larger values of γ and smallest when $\gamma \to 0$.

The behavior of the electrical analog was compared with the behavior predicted by Eq. (II.2). The device has a threshold of 19.5 V, and the drive is determined by the input current and capacitance of the RC. The RC was varied stepwise between 15 ms and 220 ms by changing capacitors. In the analog experiments, we were not able to obtain stable pulse rates down to zero imp/s as suggested by the theoretical curves, undoubtedly due to the very steep slope as s_0 $\to s_{min}$ where minute changes in drive (as occur due to noise in the analog circuit)
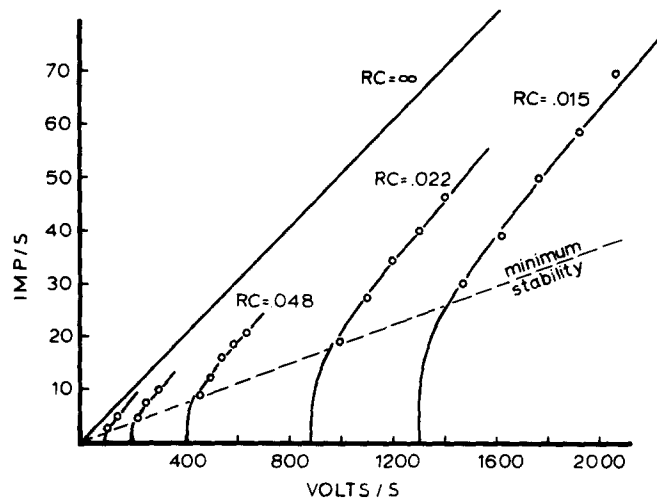
FIGURE 2.   Steady-state behavior of the leaky integrator. Pulse frequency vs. drive (s_0) in volts/second for five different settings of the leaky integrator analog (open circles). Model calculations for the same parameters used in the analog are plotted with solid lines. See text for further explanation.

represent large variations in f_0. In practice, there is a minimum stable value of f_0 for each RC setting. The dashed line drawn through these minimum stable values in Fig. 2 shows that the region of instability is larger for smaller values of RC (larger γ).

Both Fig. 2 and Eq. (II.2) (cf. Knight, 1972, Eq. [5.5]) make evident that all the response curves are simply different "magnifications" (with fixed point at the origin) of a single "universal" curve.

In summary, the steady-state behavior shows that the leak of an integrating encoder is a major factor in its performance. By varying the leak, a very wide range of steady-state behavior can be obtained.

MODULATED BEHAVIOR   The dynamic behavior of the encoder was determined by applying a sinusoidal drive of the form:

$$s_0 + s_1 \cos(\omega t + \varphi) = \frac{1}{C}[i_0 + i_1 \cos(\omega t + \varphi)], \qquad (II.5)$$

where a steady-state current i_0 is sinusoidally varied by i_1 at $f_m = \omega/2\pi$ Hz. The output function generated by this modulation is sinusoidal and to first order equals

$$f_0 + f_1 \cos(\omega t + \varphi').$$ (II.6)

The extraction of the output function from the pulse train data is discussed in Materials and Methods.

Even with rather large sinusoidal modulations, the output function shows very little distortion from a perfect sinusoid. Distortions are typically 1-4% at low modulation frequencies and somewhat higher as $f_m \rightarrow f_0$. Modulations can be increased to nearly 100% (where $f_1/f_0 = 0.5$) without significant increases in distortion, and the result appeared to hold for all values of RC (15-220 ms) tested. Perturbation theory is of no help in explaining why this is so. The perturbation expansion will not converge under these conditions, and hence does not apply. A partial answer lies in the method of analysis (binning), and in the phase-locking properties of the system in the presence of noise (see Materials and Methods). The question that remains is why does the output amplitude remain proportional to $|s_1|$ when $|s_1|$ becomes relatively large. Here the rest of the answer may lie in the nearly linear f_0 vs. s_0 steady-state relationship. However, since no closed form expression exists when $|s_1|$ is large, all neuronal data for these papers were taken with $|s_1| \lesssim 0.1\, s_0$ where perturbation theory applies.

The two gain and phase plots shown in Fig. 3 are a comparison between the behavior of the analog (closed circles) and the behavior predicted by Eq. (I.17) with $M = 1$ and $K = 0$ (solid lines). The output function in this case had a steady-state value of 30.5 imp/s with an amplitude of 1.37 imp/s at 1 Hz. As the modulation frequency is varied below 1 Hz, the phase shift is zero and the amplitude is constant. However, as ω increases toward $2\pi f_0$ the amplitude and phase both increase, such that the amplitude reaches a maximum in the neighborhood of $f_m = f_0$ and then decreases as ω is increased further. The amplitude passes through a minimum and approaches another maximum at $2f_0$. According to the model equation, this behavior repeats at each integer multiple of f_0 since the denominator term $F(0)$ of Eq. (I.20) equals zero whenever $\omega/f_0 = 2\pi l, l = 1, 2,$ 3, . . ., leading to an infinite output amplitude at these values of f_m. An infinite response of the mathematical model at these modulation frequencies corresponds in the electrical analog to a nonsinusoidal response. In fact the analog becomes phase locked, and a single pulse occurs always in the same phase relative to the modulating sinusoid. Moreover, the analog may show this behavior for a range of modulation frequencies in which f_0 is determined by ω (see Rescigno et al., 1971).[6]

Eq. (I.17) with $M = 1$ and $K = 0$ predicts: (a) that the output function f_1 is directly proportional to the amplitude of the drive s_1 for any given ω, f_0, and γ; (b) if the modulation frequency is expressed as the ratio ω/f_0, rather than just ω, the output function is determined by the ratio f_0/γ. Thus, so long as the ratio f_0/γ

---

[6] Cycle histogram plots of 1:1 phase-locked encoder behavior show that all events occur in one bin (probability density = 1) and that the probability density is zero elsewhere. Stein (1970) has shown that for converting the probability density to rate, a value of 1 corresponds to $2f_0$ imp/s rather than an infinite rate.

(or f_0 RC in the analog model) is held constant, the output behavior is invariant with respect to ω/f_0. In the analog experiments, doubling the input did indeed double the output. Fig. 4 illustrates that the analog behavior also agrees with point (*b*) above. For a given f_0, decreasing γ produces a flatter amplitude response (narrower resonance half-width) and slower initial increase in phase as the modulation frequency is increased (cf. Knight, 1973 [Fig. 4], who also predicted this narrower "half-width" effect). Similarly, with a given γ, (RC = 45 ms in the figure) the same changes are observed as f_0 is increased.

In the limiting case where $\gamma \rightarrow 0$, which is equivalent to an electrical analog with a non-leaky integrator (i.e. impedance is C only), the ω dependence is lost and the equation reduces to a simple proportionality between f and s. In this case, the output has a constant amplitude and no phase shift (Knight, 1972).
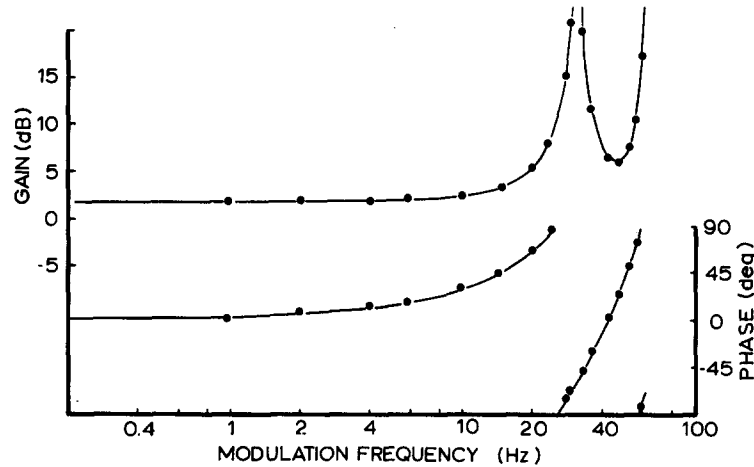
FIGURE 3. A comparison between analog simulation and mathematical equation (I.17) for the dynamic behavior of the leaky integrator model without feedback. The data points were obtained from the electrical analog and the solid lines are calculated from Eq. (I.17). Model parameters were A = 19.5 V, RC = 10 ms, f_0 = 30.5 imp/s, and s_1/s_0 = 0.00489 which were the same values used in solving the equation.

III. *Analog Behavior with Feedback*

STEADY STATE BEHAVIOR   The steady state behavior with feedback can be determined by solving Eq. (I.7) for the drive as a function of f_0:

$$s_0 = \frac{1}{1 - e^{-\gamma/f_0}} \cdot \left[A\gamma + \frac{h(e^{-1/\tau f_0} - e^{-\gamma/f_0})}{\left(\gamma - \frac{1}{\tau}\right)(1 - e^{-1/\tau f_0})} + \frac{k}{\gamma - \frac{1}{\tau_k}}(e^{-1/\tau_k f_0} - e^{-\gamma/f_0}) \right]. \quad \text{(III.1)}$$

In the limit as $\gamma \rightarrow 0$, this becomes:

$$\lim_{\gamma \rightarrow 0} s_0 = f_0 \left[A + h\tau + k\tau_k(1 - e^{-1/\tau_k f_0}) \right], \quad \text{(III.2)}$$

which approaches

$$s_0 = f_0 (A + h\tau + k\tau_k), \quad \text{(III.3)}$$

for $\tau_k \cdot f_0 \ll 1$. If one compares these equations with Eq. (II.4), one can see that for a given set of magnitude and time constant parameters, the asymptotic slope is always reduced by feedback, and it is reduced by a greater amount with summed than with nonsummed feedback. The curves in Fig. 5 are plots of Eq. (III.1) for nonsummed feedback (Fig. 5 A) and for summed feedback (Fig. 5 B). Both families of curves show the following features: (a) more drive is required to
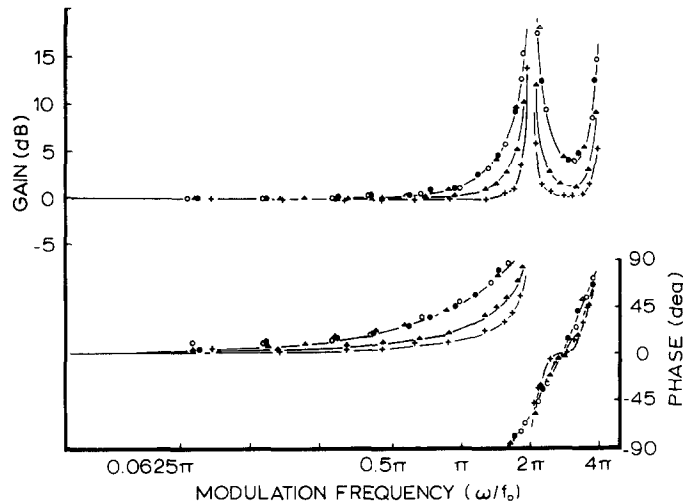

FIGURE 4. Dynamic behavior of the leaky integrator with different f_0 and RC. Symbols are data points obtained from the electrical analog and solid lines are calculations of gain and phase made from Eq. (I.19). Gain values are normalized to 0 db at 0.1 Hz and all values are plotted as a function of normalized modulation frequency, ω/f_0.

$(+)f_0 = 36$ imp/s, RC $= 45$ ms, $\gamma/f_0 = 0.62$;
$(\blacktriangle)f_0 = 17.5$ imp/s, RC $= 45$ ms, $\gamma/f_0 = 1.27$;
$(\bigcirc)f_0 = 30.5$ imp/s, RC $= 10$ ms, $\gamma/f_0 = 3.28$;
$(\bullet)f_0 = 13.8$ imp/s, RC $= 22$ ms, $\gamma/f_0 = 3.29$;
$(\triangle)f_0 = 6.8$ imp/s, RC $= 45$ ms, $\gamma/f_0 = 3.27$.

The same plots were obtained when s_1 was doubled. Thus, as predicted by Eq. (I.17), the dynamics (shape of gain curve and phase) are independent of s_1 in these normalized plots.

reach a given f_0 as feedback is added; (b) for small values of feedback time constant ($\tau \ll T$, $\tau = 25$ ms is illustrated in Fig. 5), the effects of nonsummed and summed feedback are similar; (c) compared to the no-feedback case, feedback produces a reduced early slope and lower minimum stable rate of pulse production.

For both types of feedback the effect of varying separately the magnitude and time constant has different effects on the steady-state behavior. In both cases, increasing the time constants alone produces lower minimum stable pulse rates. Further, the time constant of either type can be manipulated to obtain a nearly linear relation between f_0 and s_0 (with stable f_0 near zero), although nonsummed

feedback can achieve this with less reduction of slope than can summed feedback for any given magnitude $k(=h)$.

TRANSIENT BEHAVIOR In response to a step current the analog with summed feedback produces adaptive behavior with a pulse frequency declining exponentially to an asymptotic value $f(\infty)$. In deriving Eq. (I.12) this empirical observation was used as an underlying assumption.[3]

Fig. 6 shows a plot of pulse frequency $f - f(\infty)$ vs. time (where $f(\infty) = 24$ imp/s). In the logarithmic plot the solid line is a linear regression fit to the data points and the dashed line is drawn according to the time constant, τ_f, calculated from
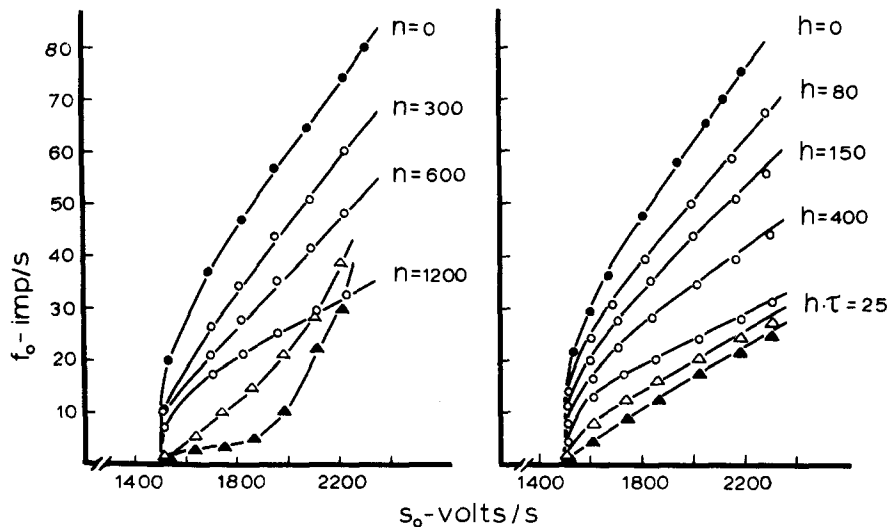
FIGURE 5. Steady-state behavior of the leaky integrator with feedback. Symbols are data points from the electrical analog and solid lines are calculations from Eq. (III.1). Model RC was 15 ms. A, Nonsummed feedback (left plot). (●) No feedback; (○) increasing values of k with $\tau_k = 25$ ms; $k = 1,200$ V/s and $\tau_k = 25$ ms (○), 100 ms (△), and 400 ms (▲). B, Summed feedback (right plot). (●) No feedback; (○) increasing values of h with $\tau = 25$ ms; (△) $h = 250$ V/s, and $\tau = 100$ ms; (▲) $h = 100$ V/s and $\tau = 400$ ms.

Eq. (I.12) with the model parameters. The model parameters used were $\gamma = 66.7$ s^{-1}, $A = 19.5$ V, $\tau = 2.5$ s, and $h/H(\infty) = 0.015$. The data indicate a value for τ_f of 0.778 s to be compared with the calculated $\tau_f = 0.746$ s. The agreement is well within the errors of estimating τ and $h/H(\infty)$ which were determined directly from measurements made from the oscilloscope face. However, they could also have been estimated from the first three intervals after the step by using Eq. (I.12) and (I.14) with the measured value of $f(\infty)$. With these equations we obtain $h/H(\infty) = 0.016$ and from the measured τ_f of 0.778 s we obtain $\tau = 2.85$ s.

Using Eq. (I.14) to determine h implies taking a small difference between the two large numbers in brackets. This invariably leads to the possibility of large errors in the determination of the value of h. Therefore the value so determined was cross-checked with that resulting from the use of Eq. (I.10).

Thus it is possible, from the response to a step input, to obtain the parameters of the summed feedback leading to the adaptation after the onset of that input. It only requires that we know A and γ. The threshold voltage (A) can be determined for a neuron by measurement or estimate and the applicable value of γ from the modulated behavior (see Fohlmeister et al., 1974a, and below).

MODULATED BEHAVIOR WITH FEEDBACK   Nonsummed feedback alone, while it alters steady-state behavior, decreases only the amplitude of the dynamic response uniformly at all modulation frequencies, and it does not affect phase. This behavior has been discussed in connection with the model after Eq. (1.19) (cf. also Discussion).
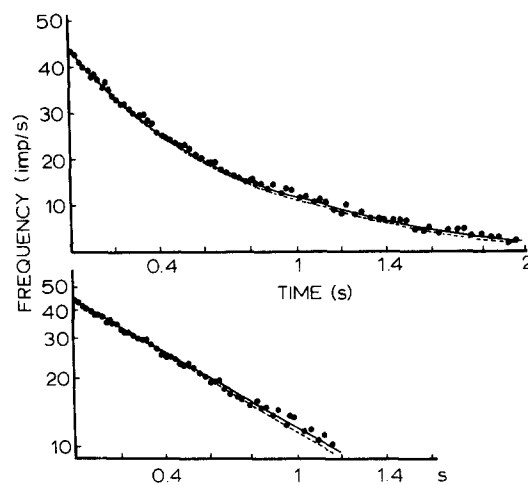
FIGURE 6.   Transient behavior of the leaky integrator with summed feedback. Symbols are data points obtained from the leaky integrator analog with $RC = 15$ ms, $h/H(\infty) = 0.015$, $\tau = 2.5$ s, and $f_0 = f(\infty) = 24$ imp/s. The frequence $[f(t) - f(\infty)] = [(\text{intervals})^{-1} - f(\infty)]$ is plotted vs. time in the upper plot, and log $(f(t) - f(\infty))$ vs. time in the lower plot. The solid line is computed by linear regression fit to data points in the lower plot and replotted in the upper plot. The dashed line is calculated from Eq. (1.12) by using the parameters of the analog.

Summed Feedback Alters Both Amplitude and Phase of the Encoder Response

At very low frequencies of modulation, summed feedback decreases the response amplitude; it has less effect at modulation frequencies near $f_0/2$ where the gain with summed feedback may either increase or decrease relative to the no feedback gain. Summed feedback again decreases the response in the neighborhood of f_0 and its multiples (see Fig. 7). The effect on phase is also confined to modulation frequencies near zero, f_0, and its multiples with zero phase shift at half-odd integer multiples of f_0. The effects of summed feedback are the result of frequency-dependent alterations introduced by the feedback term in Eq. (1.17). Since this term is a multiplicative factor to the equation without feedback, the two terms will simply add in plots on a log scale. Likewise, the phase contribution of feedback will add to the phase without feed-

back. The summation property of the gain is clearly seen in Fig. 9 (below), where the feedback term is plotted as a dotted line and the equation without feedback is the thin solid line. The heavy solid line, which represents the response of the encoder with feedback, is also the sum of the other two curves minus a constant (2.1 dB) which is the reduction in effective drive caused by the feedback.
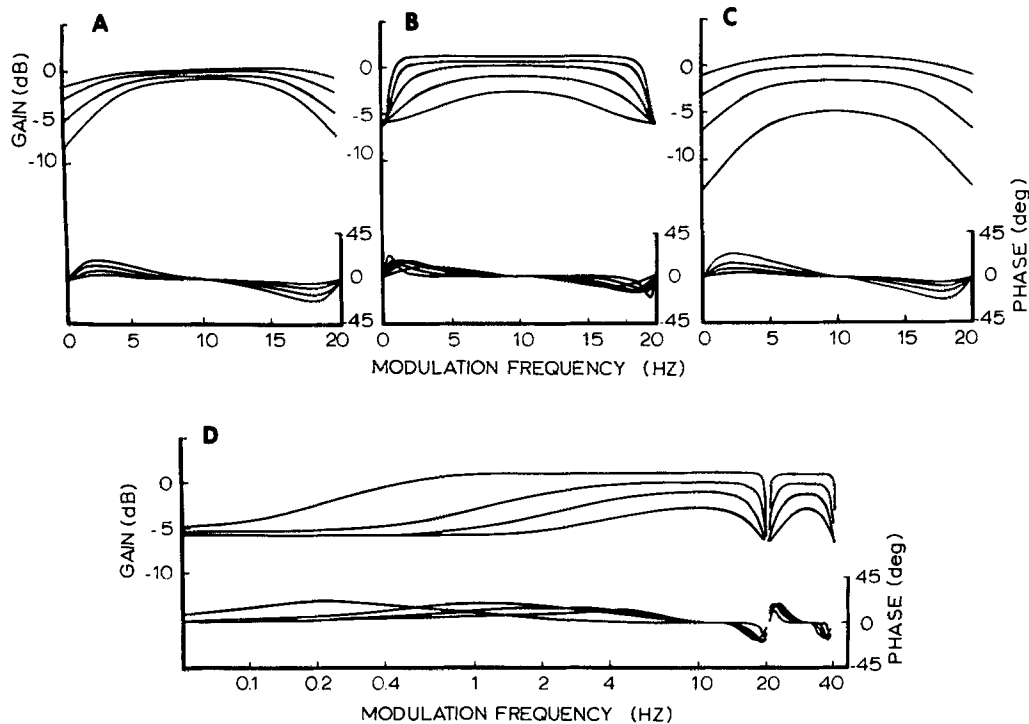
FIGURE 7.   Dynamic behavior of leaky integrator with summed feedback. Plots of feedback term in Eq. (I.17) for various parameters RC, γ, and h with f_0 = 20 imp/s. A, RC = 15 ms, τ = 100 ms, and h = 20 V/s (top curve in gain and low frequency phase), 40 V/s, 80 V/s, and 160 V/s (bottom curves). B, RC = 15 ms, $h \cdot \tau$ = 10 V with τ = 1.0 s (top curve in gain and lowest frequency peak in phase), 500 ms, 200 ms, 100 ms, and 50 ms (bottom gain curve and highest frequency peak in phase). C, τ = 100 ms, h = 40 V/s, RC = 45 ms (top curve in gain and low frequency phase), 15 ms, 10 ms, and 7.5 ms (bottom curves). D, Same as B with a logarithmic frequency scale.

The effect of the h, τ, and γ parameters on the encoder behavior is summarized in Fig. 7. Parts A–C are plotted on a linear frequency scale to emphasize that both the amplitude and phase of the feedback component are symmetrical, about $f_0/2$ (10 Hz in this case). All three factors affect the magnitude of the feedback, while only τ has a significant effect on the frequency response. Increasing any of these parameters increases the ratio between maximum and minimum of the feedback factor. However, γ alone (C) reduces both maximum

and minimum more than is achieved by increasing h alone (A). The effect of τ on the frequency response is shown in Fig. 7 B and also in Fig. 7 D, which is a plot of the same parameters on log frequency coordinates. The latter plot emphasizes the low-frequency cut-off feature of summed feedback, and shows how the cut-off varies with τ.

When both summed and nonsummed feedback are included together, it can be seen from Eq. (I.17), (I.18), and (I.19) that the nonsummed part does enter into terms that affect dynamics. This is illustrated in Fig. 8. The solid curves are gain and phase with summed feedback alone ($h = s_1, = 0.013$ V/s, and $\tau = 0.8$ s). When nonsummed feedback is added, the gain and phase become the dashed curves. The values of k and τ_k chosen for this example correspond to the
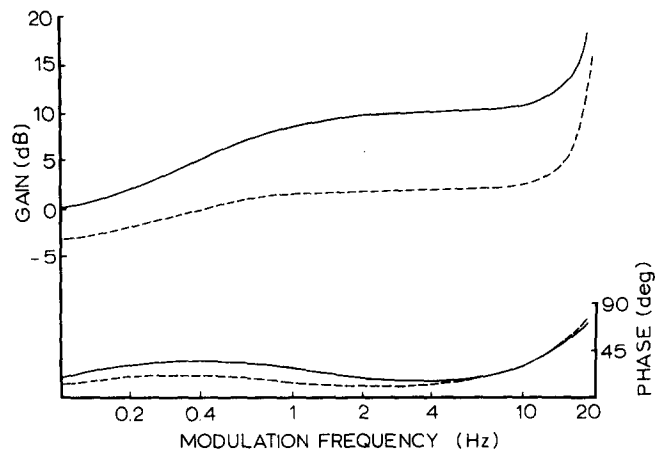

FIGURE 8. Dynamic behavior of leaky integrator with summed and nonsummed feedback together. Curves are plotted from Eq. (I.17). Solid curves: RC = 27 ms, h = 0.013 V/s, $s_1 = 0.013$ V/s, $f_0 = 20$ imp/s, $A = 5$ mV, and $k = 0$. Dashed curves, same parameters except $k = 1.0$ V/s and $\tau_k = 6.5$ ms. The solid curves are also plots of the equation with $h = 0.035$ V/s, $s_1 = 0.035$ V/s, $k = 1.0$ V/s, and $\tau_k = 6.5$ ms. The ratio $h/s_1 = 1.0$ determines the gain and phase independently of the presence of nonsummed feedback for given f_0, γ, and A.

parameters which produce a neuron-like after hyperpolarization in the potential trajectory (see also Fig. 13). However, by increasing both h and s_1 (such that $h = s_1$ = 0.035 V/s) the gain and phase revert to the solid curves. Therefore, although nonsummed feedback alone has no effect on gain or phase, it alters the effect of summed feedback when it occurs together with it. That effect is entirely on the magnitude h but not on the ratio h/s_1. Therefore, although the transfer function contains only the ratio h/s_0, it can be seen from this example that the ratio h/s_1 becomes an important parameter in determining gain and phase as we have defined them.

IV. Curve Fitting and Parameter Variation

The model presented here serves as a basis for exploring the behavior and mechanisms of repetitively firing neurons. Therefore we will attempt to corre-

late the model behavior with the responses of these neurons by specifying a set of parameters which produce a describing function that most closely matches the neuronal data. To do so requires that we have some idea about how sensitive the model equations are to variation of parameters. We explored the problem by testing our ability to fit data generated by the electrical analog using only the data obtained with a sinusoidal drive. As noted above, the transient behavior provides an additional independent measure of some of the parameters when summed feedback is present.

Four variables of the electrical analog were fixed as: $RC = 48.4 \pm 10\%$ ms, $A = 19.5$ V, $\tau = 450$ ms, $f_0 = 12.4$ imp/s. Ratios were used in setting the other
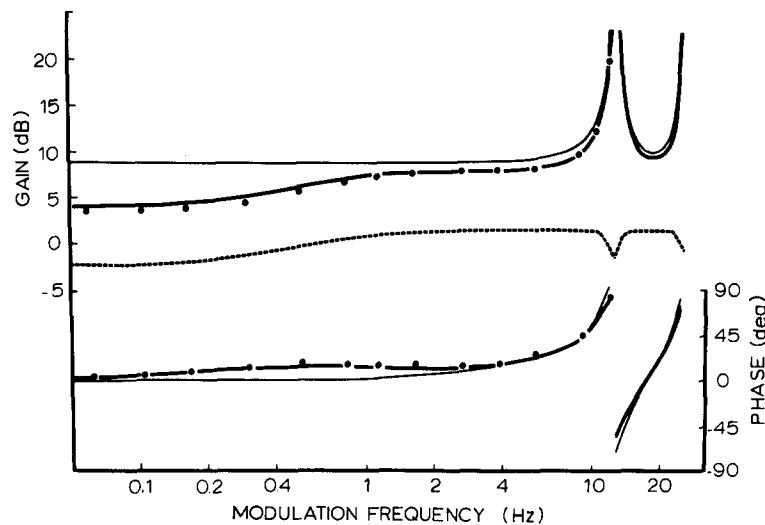

FIGURE 9. Dynamic behavior of leaky integrator with summed feedback. The symbols are data points obtained from the electrical analog with $A = 19.5$ V, $RC = 48$ ms, $f_0 = 12.4$ imp/s, $h/s_1 = 0.0361$, and $s_1/s_0 = 0.052$. The heavy solid line is a plot of Eq. (I.17) using parameters determined by a parameter variation fit to the experimental data (see text). The thin lines are plots of Eq. (I.17) (with no feedback) for the same model. The dashed line is a plot of the feedback terms only in Eq. (I.20).

parameters, such that: $A/s_0 = 31.8$ ms, $s_1/s_0 = 0.052$, and $h/s_1 = 0.0361$. Amplitude and phase data (14 points) were then taken approximately equally spaced (log scale) over a range of modulation frequencies between 0.05 Hz and 11.8 Hz (Fig. 9, closed circles). Using this data as the unknown, a simplex method of variation of parameters (Nelder and Mead, 1964) was used to find the set of parameters which gave the best root mean square fit of the experimental data to the amplitude and phase equations. Although the parameter space proved to have many local minima, it was always possible to find a best fit by adopting an appropriate strategy.[7] In this example, the experimental data were fit to ± 0.08

[7] Since we were testing a model with summed feedback only, we excluded any consideration of nonsummed feedback. Even with the remaining six parameters (Eq. [I.17]) it was not possible to let all six vary simultaneously and obtain a best fit. However, we could let two or three vary at a time and

imp/s in amplitude and $\pm 1.05°$ in phase (Fig. 9, heavy solid line). The parameters which give this fit were: $RC = 53.5$ ms, $\tau = 428.4$ ms, $A/s_0 = 33.5$ ms, $s_1/s_0 = 0.068$, and $h/s_1 = 0.0377$.

All the examples we tried were not equally successful since the ability of the technique to provide the correct parameters depended on the values of the parameters themselves (due to the exponential terms containing them), and on the range and accuracy of the data available. We found, for example, that we
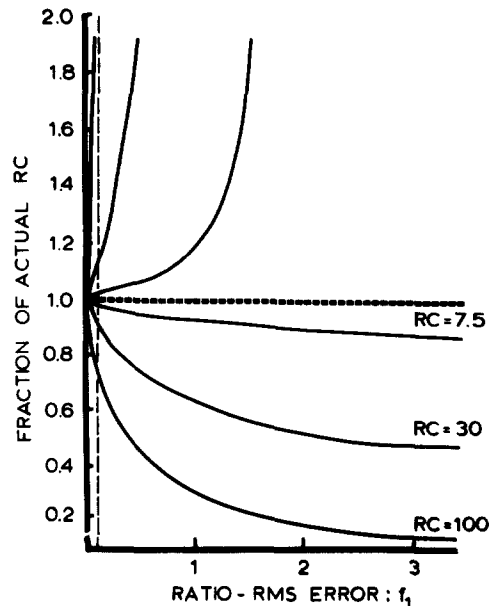

FIGURE 10. Parameter determination of γ of the leaky integrator from the gain curve. 16 data points obtained for modulation frequencies between $f_0/2$ and f_0 were subject to a variation of parameters fit to Eq. (I.20) for $f_0 = 15$ imp/s and $|f_1| = 3$ imp/s. Ordinate is the ratio of the acutal RC used to generate the data to the RC determined from the fit when the RMS error between data and equation is a given fraction of the modulation $|f_1|$ (abscissa). The dashed vertical line is drawn at 0.3 imp/s (this example) or 10% of the modulation amplitude. The curves below the horizontal dashed line are the locus of points obtained when the variation of parameters routine converges from values less than RC and the upper portions of the curves are obtained when it converges from larger values.

had better success in specifying γ if it was large since the solutions were insensitive to changes in γ when it was small. Fig. 10 illustrates the parameter sensitivity of the amplitude to variations in γ about three nominal values $\gamma = 133$ s^{-1}, $\gamma = 30$ s^{-1}, and $\gamma = 10$ s^{-1}. The variation of γ which produces a significant error is smallest for $1/\gamma = 7.5$ ms and very large for $1/\gamma = 100$ ms. Thus, when

attempt to fit certain critical parts of the amplitude and phase curves. For example, using the result that h does not greatly affect the amplitude near $f_0/2$, we started by assuming $h = \tau = 0$, and tried to fit the amplitude in the range $0.5 f_0 - 0.9 f_0$ by varying RC and s_1. The feedback parameters were then obtained by finding a best fit to the phase. Finally, the parameters were tested on the total gain and phase data.

the leak is small, data can be fit equally well with equations describing the encoder with no leak, whereas for large leaks the value of γ must be specified very precisely in order to fit data to the model.

This example gives an indication of the range of parameter sensitivity for γ. A similar dependency on parameter value was also found for τ and τ_k. However, it is not our purpose to provide here an exhaustive study of this problem, but rather to give warning of its complexity and to state that there seems to be no general method for parameter specification that will yield satisfactory results in all cases.

V. *Comparison of Leaky Integrator and Variable-γ Models with Feedback*

LOADING   As we have shown previously (Fohlmeister et al., 1974 a), the leaky integrator fails to explain many features of the dynamic behavior of sensory neurons. We have presented a model based on a time- and voltage-dependent γ which reconciles those differences. Here it is shown that the alteration in gain and phase produced by feedback in the leaky integrator are also produced in the variable-γ model. In fact the gain curves for these two models are identical. This identity allows us to define a $\bar{\gamma}$ of the variable-γ model for the conditions of each Bode plot. The $\bar{\gamma}$ is defined to equal the leaky integrator γ used in generating the same gain curve. This is a useful tool because the determination of $\bar{\gamma}$ is independent of the value of threshold as well as the shape and nature (i.e. summed feedback or not) of the drive.

The phase curves of the leaky integrator and variable-γ models correspond only in the low frequency range (modulation frequencies $<f_0/4$). In this frequency range the phase curve is in fact model independent and zero in the absence of summed feedback. In the presence of summed negative feedback the low frequency phase becomes non-zero and positive, but the resulting shape remains model independent (Fig. 11). The magnitudes of the shift however become equal only if the gain curves are first superimposed — i.e. only if $\bar{\gamma}$ is first made to match the leaky integrator γ. This implies that the low frequency phase is a measure of the "average" loading, but not of the functional details of the load.

STEADY-STATE BEHAVIOR OF VARIABLE-γ WITH FEEDBACK   It has been pointed out that the steady-state f_0 vs. i_0 behavior of sensory cells such as the crayfish stretch receptor is very linear and that these cells are capable of steady-state firing rates at very low frequency (<1 imp/s) (e.g., Terzuolo and Washizu, 1962). The leaky integrator even with summed feedback does not mimic this behavior very well. The variable-γ, however, does give a nearly proportional f_0 vs. s_0 behavior (Fig. 12). This is due to the fact that for each f_0 there is a different $\bar{\gamma}$ such that $\bar{\gamma}/f_0 \cong$ constant. Rewriting Eq. (II.2) in the form

$$ln\left(1 - \frac{\bar{\gamma}A}{s_0}\right) = -\bar{\gamma}/f_0 \qquad\qquad (V.1)$$

leads to

$$s_0 = \frac{\bar{\gamma}A}{1 - \exp\left(-\bar{\gamma}/f_0\right)}, \qquad\qquad (V.2)$$

upon taking the exponential of both sides. With $\bar{\gamma}$ approximately proportional to f_0 this results in

$$s_0 \doteq \text{constant} \cdot f_0. \tag{V.3}$$

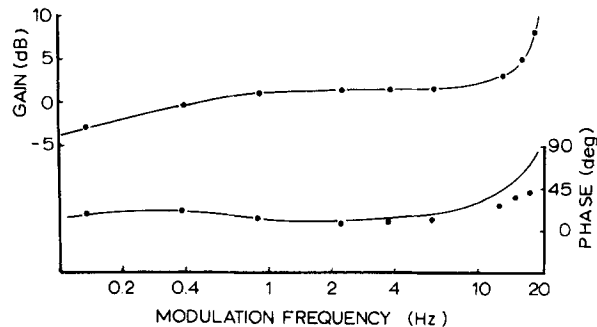This property continues to hold in the presence of summed feedback. The total

FIGURE 11. Dynamic behavior of the variable-γ model with summed feedback compared to the leaky integrator. The points are values computed for the variable-γ model with $A = 8$ mV, $B = 0.2$ s^{-1}, $D = 0.00015$ s^{-2}-V^{-1}, γ (0) $= 0.35$ s^{-1} (giving a value of $1/\bar{\gamma} = 27$ ms; see Fohlmeister et al., 1974a), $h = 0.02$ V/s, $s_1 = 0.02$ V/s. $\tau = 0.8$ s, $s_0 = 0.64$ and therefore $f_0 = 20$ imp/s. The solid curves are drawn from a solution of Eq (I.17) with $A = 8$ mV, $1/\gamma = 27$ ms, $h = 0.0076$ V/s, $\tau = 0.8$ s, $s_1 = 0.0076$, $s_0 = 0.4711$ and $f_0 = 20$ imp/s. The h/s_1 ratio, τ, and γ are the same for the two models.
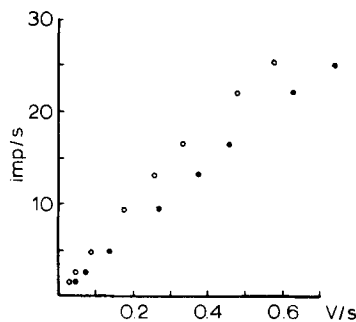

FIGURE 12. Steady-state behavior of the variable-γ model. Open circles are for the same model parameters used in Fig. 11 without feedback and the closed circles are with summed feedback.

amount of summed feedback effect H subtracts from the applied stimulus s_0 (Eq. [I.9]). In the steady state, $H(\infty)$ is always proportional to f_0 (Eq. [I.10]). Mathematically, these two statements imply that s_0 is to be replaced by $s_0 - H(\infty)$ everywhere it appears in Eq. (V.1), (V.2), and (V.3). It follows that Eq. (V.3) retains its form in the presence of feedback with the value of the constant increased by the added amount $h \cdot \tau$.

INTERSPIKE VOLTAGE TRAJECTORIES   One of the attractive aspects of the variable-γ model is that interspike voltage trajectories are similar to what is

observed intracellularly in sensory neurons. In particular there is an afterpotential after each spike followed by a near linear rise to threshold. In the variable-γ model this is the result of a time-varying membrane load that initially drives the voltage toward the potassium equilibrium potential. But it is clear that a similar potential trajectory could also be generated by nonsummed feedback with appropriate choice of k and τ_k. This is shown in Fig. 13. The dashed potential curve was generated by the variable-γ model and the solid curve by the leaky integrator with $k = 1.0$ V/s and $\tau_k = 0.0065$ s. The gain and phase curves for
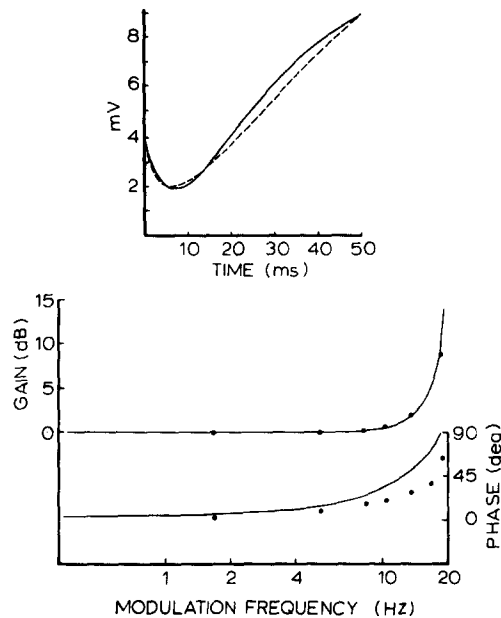
FIGURE 13. Comparison of the variable-γ model with the leaky integrator with nonsummed feedback. Upper plot shows the voltage trajectory of the variable-γ model for the parameters used in Fig. 11 (dashed curve) and of the leaky integrator model with RC $= 27$ ms, $k = 1.0$ V/s, $\tau_k = 6.5$ ms, and $f_0 = 20$ imp/s. Bode plot shows the gain and phase computed for the two models; solid line; leaky integrator (Eq. [1.17]) and points, variable-γ model.

these models are plotted below. Notice that the gain curves are identical, indicating that the average loading is the same for the two models. In the one case, however, the trajectory shape is due to effective changes in the stimulus and in the other to changes in loading. To decide which of the two mechanisms is responsible for the trajectory we refer to the phase data which show that when a particular voltage trajectory is caused by time-dependent changes in drive, the phase is identical to the phase of the leaky integrator. This is entirely consistent with our earlier observation that the phase curve is particularly sensitive to the precise membrane loading in the interspike interval. Therefore we caution that models which attempt to fit only voltage trajectories may not be sufficient to account for the dynamic behavior of the encoder.

DISCUSSION

The principal results of this paper are: (a) a verification of the mathematical analysis of the leaky integrator model using an electrical analog with known parameters; and (b) the demonstration that the parameters of summed feedback can be determined from Bode data for the leaky integrator and for the more general variable-γ model.

The first result gives confidence in the use of the small perturbation technique used in the mathematical derivation of the gain and phase equations and also confirms the appropriateness and accuracy of the interval binning technique used to handle experimental data.

The second result bears directly on the problem posed in the companion paper (Fohlmeister et al., 1977): the determination of feedback parameters in two sensory neurons. We showed that it is possible to determine accurately a number of model parameters for the leaky integrator model from the gain and phase. Specifically, the model value of γ can be determined from the gain data to within less than $\pm 10\%$ for values of 33 s^{-1} or greater (see Fig. 10), and this includes the range of values of $\bar{\gamma}$ found for sensory neurons (Fohlmeister et al., 1974a; 1977). Furthermore, such determination is independent of the presence of feedback. When feedback is present it is additionally possible to determine the parameters of summed feedback but not of the nonsummed variety, since only summed feedback has an effect on the dynamics. Steady-state behavior can only suggest a contribution by feedback and cannot at present be used reliably to determine its parameters.

As long as it is possible to determine a $\bar{\gamma}$ from the gain curve produced by a particular encoder, the results of the analysis with both summed and non-summed feedback operating together as well as those with the variable-γ model suggest that it is always possible to determine the ratio h/s_1 and the time constant τ from the gain and phase. For instance, when the $\bar{\gamma}$ for the variable-γ equals γ for the leaky integrator, the low-frequency gain and phases are identical in the two models when the same values of h/s_1 and τ are used (Fig. 11). So even if one questions the appropriateness of the variable-γ as a relatively accurate neuron model, there is some basis for confidence in the determination of neuronal feedback from a sinusoidal analysis because that determination appears to be model independent.

Even though it is the ratio h/s_0 that appears in the transfer function (Eq. [1.17]), the results show that the dynamic behavior of $|f_1|$ for a given f_0 varies with the parameter $|s_1|$, the magnitude of the sinusoidal component of encoder drive. Thus, in order to know the magnitude of encoder feedback h, it is necessary to know also the magnitude of drive effective at the encoder site. With that information, then, it is possible to determine both the magnitude and the time constant of summed feedback for an encoder from spike train analysis by using the leaky integrator model as a basis for the determination.

As for the nonsummed feedback, it does not seem that its presence can be established in a general or model-independent sense. In the context of the leaky integrator it may be identified and evaluated by comparing the value of appar-

ent RC from the steady behavior with the γ determined from the gain curve; a discrepancy may indicate the presence of a nonsummed effect. In this context, we have shown that such nonsummed effects can produce charging curves in the interspike interval that are similar to those observed in many repetitively firing neurons. By using a large k and small τ_k the voltage trajectory exhibits an afterhyperpolarization even with a constant RC load and a constant stimulus s_0, because the drive now becomes $s_0 - k \exp (-t/\tau_k)$ after each spike (Fig. 13). A dynamic analysis of this system, however, yields a phase curve identical with the no-feedback case ($k = 0$) which differs substantially from the ω-dependence of sensory neurons which exhibit an afterhyperpolarization (Fohlmeister et al., 1974a). This result, of course, does not preclude the existence of a nonsummed feedback effect; it does, however, support the need for a variable load in order to mimic the dynamic behavior of certain neurons and it is therefore unlikely that nonsummed feedback in the drive is responsible for the shape of the charging curve in those cases.

In the steady state and in the transient equations, threshold potential A appears explicitly. Further, in the derivation of the modulated behavior, integrals appear whose value depends on threshold. In these derivations we implied that A is a fixed number. The assumption of a fixed threshold is probably justified for the steady-state case and fairly accurate for the modulated case, since the encoder is assumed to have been operating with a stimulus near a constant value s_0 for an indefinitely long time. Thus, since the interspike intervals are all nearly identical, the neuronal encoder is presumably experiencing nearly the same threshold at the time of each impulse occurrence. For the transient behavior A may not be constant and the relative significance of any threshold increase must be evaluated with each individual situation. Effects that threshold variations can introduce into encoder dynamics are considered in detail elsewhere (see footnote 3).

The appendix contains the derivation of two transfer functions—both with two channels of feedback. The first contains one channel of summed and one channel of nonsummed feedback. The second contains two channels of summed feedback for comparison with the sensory neurons (studied in Fohlmeister et al., 1977) which appear to operate with two such mechanisms that have widely different decay times. In each channel the feedback effect increases by a fixed amount (h or k) in response to an impulse, followed by a relaxation of the effect which is approximated by an exponential decay. The possibility of a delay between the spike and the onset of feedback is not considered here. This problem has been discussed by Ratliff et al. (1969) and by Purple and Salasin (1969).

The model studies illustrate two important points pertaining to information processing in the leaky encoder. While requiring a greater drive than the nonleaky integrator, the leaky encoder also confers a greater, absolute, static gain (sensitivity in terms of impulses/s/Δs_0) which may, over certain ranges of drive, be linearized by the presence of feedback (Fig. 5). Second, the phase-locking properties of these models cause the dynamic sensitivity (frequency response) to increase as the input frequencies ω approach the mean rate of firing

f_0.[8] With regard to the first point one might speculate that the linearized, enhanced gain requires fewer signal channels to carry a given signal/noise level to the next neurons in a circuit. On the second point, encoder frequency enhancement could be a mechanism utilized by the nervous system to achieve enhanced sensitivity to certain time-varying changes in the environment. Other possible utilities relating to phase locking, re-entrant patterns, and stability with respect to noise have been discussed by Stein (1970), Stein and French (1970), Knight (1972), and Rescigno et al. (1970). Such nonlinear behavior, as exhibited by the leaky encoders, suggests that the encoder process in a neuron is an important mechanism in the further integration and processing of information within the repetitively firing nerve cell.

APPENDIX

In the course of the Results we make extensive reference to the effects of summed and nonsummed feedback on the dynamic properties of impulse encoding. For the purposes of these papers we derive here two transfer functions. Both derivations utilize first-order perturbation theory within the context of the leaky integrator. For the first we assume simultaneously one channel of summed and one channel of nonsummed feedback.

Second, we derive the transfer function with two simultaneous summed feedback channels in order to have an expression of channel crosstalk for these dynamically important feedbacks.

The complex number notation in the sinusoidally perturbed stimulus $s(t) = s_0 + s_1 \exp (j\omega t)$, (Eq. [I.16]), allows both amplitude (gain) and relative phase shift to be computed in compact form. The constant s_1 is in general complex, its argument giving the arbitrary phase of the stimulus sinusoid at the lower limit, $t = 0$, of the integral for A (Eq. [I.6]), that is, at the beginning of the interspike interval.

Including the perturbation term s_1 in the integral Eq. (I.6) now renders closed-form mathematics intractable. The approximation used to bypass this difficulty is to assume all perturbation terms (that is terms with subscript 1) to be a small fraction, $\leq 20\%$ of the steady-state values (subscript 0), of the corresponding variables. This approximation can always be satisfied experimentally by an appropriately "small" choice of the magnitude $|s_1|$. With this approximation, terms involving products of two or more factors of the perturbing quantities may be neglected in comparison with terms containing only one such factor. This procedure, known as first-order perturbation theory, is eminently adequate for the identification and determination of feedback parameters as shown below. The function so derived contains full transfer information, provided that it is compared with experiments utilizing a sinusoidal perturbing stimulus of sufficiently "small" amplitude (see Discussion).

The integral, Eq. (I.6), including the sinusoidal perturbation of Eq. (I.16), now takes the form:

$$A = \int_0^T dt \; e^{-(T-t)\gamma}\{s_0 + s_1 e^{j\omega t} - ke^{-t/\tau_k} -h \sum_{m=0}^{\infty} e^{-(\hat{T}(m,\omega,T_0)+t)/\tau}\}. \tag{A.1}$$

The interpulse period is generalized to $T = T_0 + T_1$, with T_1 the (complex) perturbation in period.

To calculate the factor $\hat{T}(m, \omega, T_0)$, which is the time interval between the occurrence of

---

[8] For a single neuron this obtains by choosing the appropriate ω-dependent normalization, Eq. (A-13). In treating a large population of neurons, the normalization is implicit (Knight, 1972). This results in the so-called resonance behavior.

the mth pulse before that at $t = 0$, and time $t = 0$, we need to determine the behavior of the T_1 term as a function of time (cf. also Knight, 1969). The magnitude and phase of T_1 depends on the magnitude and phase of s_1. Further, since s_1 varies sinusoidally, the T_1 perturbation term will also vary periodically in time with the same frequency ω. Therefore, the perturbation term of m periods before the present integration interval takes the form $T_1 e^{-jm\omega T_0}$. The T_0 in the exponent, in place of a more general T, is consistent with the first-order perturbation approximation.

The summed feedback term in Eq. (A.1) contains an infinite series — the total feedback from an infinite number of previous pulses remaining at $t = 0$. From the discussion in the previous paragraph the factor $\hat{T}(m, \omega, T_0)$ becomes

$$\hat{T}(m, \omega, T_0) \doteq mT_0 + T_1 \sum_{r=1}^{m} e^{-jr\omega T_0} = mT_0 + T_1 \frac{1 - e^{-jm\omega T_0}}{e^{j\omega T_0} - 1} . \tag{A.2}$$

The integral of Eq. (A.1), because it involves an imaginary exponential as well as a complex s_1 and complex T_1 is a contour integral in the complex-t-plane. However since the integrand is an analytic, entire function with a pole only at infinity, the integral may be treated as any real variable integration. Integrating term by term, the first two terms are

$$\int_0^T dt(s_0 + s_1 e^{j\omega t})e^{(t-T)\gamma} \doteq \frac{s_0}{\gamma} (1 - e^{-T\gamma}) + \frac{s_1}{j\omega + \gamma} (e^{j\omega T_0} - e^{-\gamma T_0}). \tag{A.3}$$

Note that — consistent with the first-order perturbation approximation — the interspike period in the s_1 integral has been replaced by T_0. Expanding the T_1 portion of the exponential in the s_0 term,

$$\frac{s_0}{\gamma} [1 - (1 - T_1\gamma + \cdots)e^{-T_0\gamma}], \tag{A.4}$$

and again retaining only zero- and first-order terms results in the integrated value of Eq. (A.3):

$$\frac{s_0}{\gamma} (1 - e^{-T_0\gamma}) + s_0 T_1 e^{-T_0\gamma} + \frac{s_1}{j\omega + \gamma} (e^{j\omega T_0} - e^{-T_0\gamma}). \tag{A.5}$$

Integration of the nonsummed feedback term is similar to the s_0 integration and leads to the contributions

$$-k \int_0^T dt \, e^{-(T-t)\gamma}e^{-t/\tau_k} \doteq - \frac{k\tau_k}{\gamma\tau_k - 1}(e^{-T_0/\tau_k} - e^{-T_0\gamma})$$
$$+ T_1 \frac{k}{\gamma\tau_k - 1}(e^{-T_0/\tau_k} - \gamma\tau_k e^{-T_0\gamma}). \tag{A.6}$$

The summed feedback term has the following form (cf. Eq. [A.2]):

$$-h \sum_{m=0}^{\infty} \exp \left\{ -\left[mT_0 + T_1 \frac{1 - e^{-jm\omega T_0}}{e^{j\omega T_0} - 1} \right] \frac{1}{\tau} \right\} \cdot \int_0^T dt \, e^{-t/\tau}e^{-(T-t)\gamma}. \tag{A.7}$$

The T_1 exponential factor is expanded to yield

$$-h \sum_{m=0}^{\infty} e^{-mT_0/\tau} \left(1 - \frac{T_1}{\tau} \cdot \frac{1 - e^{-jm\omega T_0}}{e^{j\omega T_0} - 1} + 0 \, (T_1^2) \right) \int_0^T dt \, e^{-t/\tau} \, e^{-(T-t)\gamma}. \tag{A.8}$$

Retaining only terms up to first order in T_1 the summation is that of two geometric series:

$$-h\left(1 - \frac{T_1}{\tau}\frac{1}{e^{j\omega T_0} - 1}\right)\sum_{m=0}^{\infty}e^{-mT_0/\tau} - \frac{hT_1}{\tau}\frac{1}{e^{j\omega T_0} - 1}\sum_{m=0}^{\infty}e^{-m\left(\frac{1}{\tau} + j\omega\right)T_0}$$

$$= -h\left(1 - \frac{T_1}{\tau}\frac{1}{e^{j\omega T_0} - 1}\right)\frac{1}{1 - e^{-T_0/\tau}} - \frac{hT_1}{\tau}\frac{1}{e^{j\omega T_0} - 1}\frac{1}{1 - e^{-\left(\frac{1}{\tau} + j\omega\right)T_0}},$$

$$\text{(A.9)}$$

and the summed feedback term, Eq. (A.7), equals

$$-\frac{h\tau}{\gamma\tau - 1}\frac{1}{1 - e^{-T_0/\tau}}\left[e^{-T_0/\tau} - e^{-T_0\gamma} - T_1\left(\frac{1}{\tau}e^{-T_0/\tau} - \gamma e^{-T_0\gamma}\right)\right]$$

$$+ \frac{T_1 h}{\gamma\tau - 1}\frac{1}{1 - e^{-T_0/\tau}}\frac{1}{e^{-j\omega T_0} - e^{T_0/\tau}}(e^{-T_0/\tau} - e^{-T_0\gamma}).$$

$$\text{(A.10)}$$

Next we add the integrated contributions (Eq. [A.5], [A.6], and [A.10]) to Eq. (A.1) and subtract from that equation the steady-state Eq. (I.7), thus:

$$0 = T_1 s_0 e^{-T_0\gamma} + \frac{s_1}{j\omega + \gamma}\left(e^{j\omega T_0} - e^{-T_0\gamma}\right) + \frac{T_1 k}{\gamma\tau_k - 1}\left(e^{-T_0/\tau_k} - \gamma\tau_k e^{-T_0\gamma}\right)$$

$$+ \frac{T_1 h}{\gamma\tau - 1}\frac{e^{-T_0/\tau} - \gamma\tau e^{-T_0\gamma}}{1 - e^{-T_0/\tau}} + \frac{T_1 h}{\tau\gamma - 1}\frac{1}{1 - e^{-T_0/\tau}}\frac{1}{e^{-j\omega T_0} - e^{T_0/\tau}}(e^{-T_0/\tau} - e^{-T_0\gamma}).$$

$$\text{(A.11)}$$

At this point we note that for

$$\frac{1}{T} = \frac{1}{T_0 + T_1} = \frac{1}{T_0} - \frac{T_1}{T_0^2} + 0\ (T_1{}^2),$$

$$\text{(A.12)}$$

we make the identifications

$$f_0 = \frac{1}{T_0}$$

$$\text{(A.13)}$$

and

$$T_1 = -f_1 T_0^2 \equiv -\frac{f_1}{f_0{}^2}.$$

$$\text{(A.14)}$$

The gain and phase curves are used primarily for the accurate determination of parameters. In particular the gain function at the higher frequencies is a sensitive measure of γ. We have found that by choosing the appropriate, frequency-dependent normalization, one can achieve a greater spacing between curves derived for two slightly different values of γ, thereby reducing error in measurement. The appropriate factor has the function of fixing the modulation wavelength so that it appears to be independent of ω. This is equivalent to normalizing the impulse frequency f_0 such that a fixed number of spikes occurs in each period of the sine wave for a given f_0. Such a normalization does change the shape of the gain and phase curves so that the gain appears to have a singularity at $\omega = 2\pi f_0$. From the shape of the gain function in the neighborhood of this infinity, one can then make precise determinations of γ. Although the frequency-dependent normalization factor applies directly to the transfer function, it may be introduced by writing a normalized perturbation frequency f_1 such that

$$f_1 \equiv \frac{1 - e^{-j\omega/f_0}}{-j\omega/f_0}f_1{}^{\text{unnormalized}}.$$

$$\text{(A.15)}$$

Substituting (A.14) and (A.15) for T_1 in Eq. (A.11), we solve for f_1/s_1 which is the transfer

function (I.17).[9] To extract the gain and phase from this expression one defines Gain $=$ 20 log $|f_1/s_1|$, and calculates Phase $=$ Arctan $[Im\ (f_1/s_1)/Re\ (f_1/s_1)]$ (cf. Results).

With two summed feedbacks the leaky integrator charging curve becomes

$$\dot{u} = -\gamma u + s_0 + s_1\ e^{j\omega t} - H_1 - H_2, \tag{A.16}$$

where

$$H_1 + H_2 = h_1 \sum_{m=0}^{\infty} e^{-\hat{t}/\tau_1} + h_2 \sum_{m=0}^{\infty} e^{-\hat{t}/\tau_2}. \tag{A.17}$$

The integration of the feedback terms is similar to that of (A.8) and (A.9), and of the stimulus terms to (A.5), resulting in

$$\frac{s_1}{j\omega + \gamma} (e^{j\omega T_0} = e^{-\gamma T_0}) + T_1 \left\{ s_0\ e^{-\gamma T_0} - \sum_{i=1}^{2} \frac{\hat{h}_i\ \hat{\Omega}_i}{\gamma\tau - 1} \left(e^{-T_0/\tau_i} - e^{-\gamma T_0} \right) \right.$$
$$\left. + \sum_{i=1}^{2} \frac{\hat{h}_i}{\gamma\tau_i - 1} \left(e^{-T_0/\tau_i} - \gamma\tau_i\ e^{-\gamma T_0} \right) \right\} = 0; \tag{A.18}$$

analogous to (A.11). In (A.18) and the following we define

$$\hat{h}_i \equiv \frac{h_i}{1 - e^{-T_0/\tau_i}}, \tag{A.19}$$

and

$$\hat{\Omega}_i \equiv \frac{1}{1 - e^{-\left(j\omega - \frac{1}{\tau_i}\right)/f_0}}. \tag{A.20}$$

Again making the substitutions (A.14) and (A.15) in Eq. (A.18) leads to the transfer function for two summed feedbacks:

$$\frac{f_1}{s_1} = \frac{f_0}{s_0} \frac{j\omega}{j\omega + \gamma} \frac{(1 - e^{(j\omega + \gamma)/f_0})}{(1 - e^{j\omega/f_0})} \frac{1}{D\ (\hat{\Omega})} \tag{A.21}$$

where

$$D(\hat{\Omega}) \equiv -1 - \frac{\hat{h}_1\ \hat{\Omega}_1}{\gamma\tau_1 - 1} \left(1 - e^{\left(\gamma - \frac{1}{\tau_1}\right)/f_0} \right) - \frac{\hat{h}_2\ \hat{\Omega}_2}{\gamma\tau_2 - 1} \left(1 - e^{\left(\gamma - \frac{1}{\tau_2}\right)/f_0} \right)$$
$$+ \frac{\hat{h}_1}{s_0} \frac{\left(\tau_1\gamma - e^{\left(\gamma - \frac{1}{\tau_1}\right)/f_0} \right)}{\gamma\tau_1 - 1} + \frac{\hat{h}_2}{s_0} \frac{\left(\tau_2\gamma - e^{\left(\gamma - \frac{1}{\tau_2}\right)/f_0} \right)}{\gamma\tau_2 - 1}. \tag{A.22}$$

In order to determine the two summed feedbacks gain[10]

$$\left| \frac{f_1}{s_1} \right| = \frac{f_0}{s_0} \frac{\omega}{\sqrt{\omega^2 + \gamma^2}} \left[\frac{F(\gamma/f_0)}{F(0)} \right]^{1/2} [D^* \cdot D]^{-1/2}, \tag{A.23}$$

we must calculate D^*D (an asterisk [*] denotes complex conjugation). All ω-dependence is in the factors $\hat{\Omega}_i$ of Eq. (A.22) which we rewrite

[9] The transfer function $H(\omega)$ is defined for a sinusoidal forcing function such that $f_1 = H(\omega)s_1\ e^{j\omega/f_0}$. The normalized f_1 (Eq. [A.15]) includes a multiplicative factor, $e^{-j\omega/f_0}$, such that the ratio $f_1/s_1 = H(\omega)$ is in fact the transfer function. Its application is thus restricted to sinusoidal forcing functions.
[10] As defined in Results, $F(x) = e^{2x} + 1 - 2e^x \cos \omega/f_0$.

$$D = a + b\ \hat{\Omega}_1 + c\ \hat{\Omega}_2, \tag{A.24}$$

where

$$a \equiv -1 + \frac{\hat{h}_1}{s_0} \frac{\left(\gamma\tau_1 - e^{\left(\gamma - \frac{1}{\tau_1}\right)/f_0}\right)}{\gamma\tau_1 - 1} + \frac{\hat{h}_2}{s_0} \frac{\left(\gamma\tau_2 - e^{\left(\gamma - \frac{1}{\tau_2}\right)/f_0}\right)}{\gamma\tau_2 - 1}, \tag{A.25}$$

$$b \equiv -\frac{\hat{h}_1}{s_0} \frac{\left(1 - e^{\left(\gamma - \frac{1}{\tau_1}\right)/f_0}\right)}{\gamma\tau_1 - 1}, \tag{A.26}$$

$$c \equiv -\frac{\hat{h}_2}{s_0} \frac{\left(1 - e^{\left(\gamma - \frac{1}{\tau_2}\right)/f_0}\right)}{\gamma\tau_2 - 1}. \tag{A.27}$$

With these definitions

$$D^*D = a^2 + b^2\ \hat{\Omega}_1^*\ \hat{\Omega}_1 + c^2\hat{\Omega}_2^*\hat{\Omega}_2$$
$$+ ab\ (\hat{\Omega}_1 + \hat{\Omega}_1^*) + ac\ (\hat{\Omega}_2 + \hat{\Omega}_2^*) + bc\ (\hat{\Omega}_1^*\hat{\Omega}_2 + \hat{\Omega}_1\hat{\Omega}_2^*), \tag{A.28}$$

showing the type of cross-talk expected in the ω-dependence of the gain.

For the two summed feedbacks phase

$$\text{phase} = \text{Arctan}\frac{Im\ f_1/s_1}{Re\ f_1/s_1}, \tag{A.29}$$

we calculate

$$\frac{Im\ f_1/s_1}{Re\ f_1/s_1} = \frac{Im\ \{j\ (-j\omega + \gamma)(1 - e^{(j\omega+\gamma)/f_0})(1 - e^{-j\omega/f_0})\ D^*\}}{Re\ \{j(-j\omega + \gamma)(1 - e^{(j\omega+\gamma)/f_0})(1 - e^{-j\omega/f_0})\ D^*\}}$$

$$= \frac{\omega\ [Im\ U \cdot Re\ D^* + Re\ U \cdot Im\ D^*] + \gamma\ [Re\ U \cdot Re\ D^* - Im\ U \cdot Im\ D^*]}{\omega\ [Re\ U \cdot Re\ D^* - Im\ U \cdot Im\ D^*] - \gamma\ [Re\ U \cdot Im\ D^* + Im\ U \cdot Re\ D^*]}, \tag{A.30}$$

where

$$Re\ U = (1 - e^{\gamma/f_0})\ F\ (0)/2, \tag{A.31}$$

$$Im\ U = (1 - e^{\gamma/f_0})\ \sin\ \omega/f_0, \tag{A.32}$$

$$Re\ D^* = a + \frac{b}{F\ (1/\tau_1 f_0)} + \frac{c}{F\ (1/\tau_2 f_0)} - \left[\frac{be^{1/\tau_1 f_0}}{F\ (1/\tau_1 f_0)} + \frac{ce^{1/\tau_2 f_0}}{F\ (1/\tau_2 f_0)}\right]\cos\ \omega/f_0, \tag{A.33}$$

and

$$Im\ D^* = -\left[\frac{be^{1/\tau_1 f_0}}{F\ (1/\tau_1 f_0)} + \frac{ce^{1/\tau_2 f_0}}{F\ (1/\tau_2 f_0)}\right]\sin\ \omega/f_0. \tag{A.34}$$

REFERENCES

ADRIAN, E. D. 1928. The Basis of Sensation. The Action of Sense Organs. Christophers, London.

BARBI, M., V. CARELLI, C. FERIANI, and D. PETRACCHI. 1975. The self-inhibited leaky integrator: transfer functions and steady state relations. *Biol. Cybern.* **20:**51–59.

BAYLY, E. J. 1968. Spectral analysis of pulse frequency modulation in the nervous system. *IEEE Trans. Bio-Med. Engrs.* **15:**257–265.

FOHLMEISTER, J. 1973. A model for phasic and tonic repetitively firing neuronal encoders. *Kybernetik.* **13:**104–112.

FOHLMEISTER, J. F., R. E. POPPELE, and R. L. PURPLE. 1974*a.* Repetitive firing: dynamic behavior of sensory neurons reconciled with a quantitative model. *J. Neurophysiol.* **37:**1213–1227.

FOHLMEISTER, J. F., R. E. POPPELE, and R. L. PURPLE. 1974*b.* Frequency domain analysis as a means for determining variables responsible for repetitive firing. Biophysics Abstracts. *Fed. Proc.* **33:**1266.

FOHLMEISTER, J. F., R. E. POPPELE, and R. L. PURPLE. 1974*c.* Evidence for a time varying process that determines membrane conductance in the interspike interval. *Soc. Neurosci. Abstr.* **4:**211.

FOHLMEISTER, J. F., R. E. POPPELE, and R. L. PURPLE. 1975. Determination of neuronal feedback parameters from spike train analysis. *Neurosci. Abst.* **1:**680.

FOHLMEISTER, J. F., R. E. POPPELE, and R. L. PURPLE. 1977. Repetitive firing: a quantitative analysis of the encoder behavior of the slowly adapting stretch receptor of crayfish and the eccentric cell of *Limulus. J. Gen. Physiol.* **69:**849–877.

FRENCH, A. S., and R. B. STEIN. 1970. A flexible neuronal analog using integrated circuits. *IEEE Trans. Bio-Med. Engrs.* **17:**248–253.

KARMEN, T., and M. A. BOIT. 1940. Mathematical Methods in Engineering. McGraw-Hill Book Publishing Company, New York. 335.

KATZ, B. 1939. Electric Excitation of Nerve. A Review. Oxford University Press, London.

KERNELL, D. 1968. The repetitive discharge of a simple neurone model compared to that of spinal motoneurons. *Brain Res.* **11:**685–687.

KERNELL, D., and H. SJÖHOLM. 1972. Motoneurone models based on "voltage clamp equations" for peripheral nerve. *Acta Physiol. Scand.* **86:**546–562.

KERNELL, D., and H. SJÖHOLM. 1973. Repetitive impulse firing: comparisons between models based on "voltage clamp equations" and spinal motoneurons. *Acta Physiol. Scand.* **87:**40–56.

KNIGHT, B. W. 1969. Frequency response for sampling integrator and for voltage to frequency converter. *In* Systems Analysis in Neurophysiology. C. A. Terzuolo, editor. University of Minnesota, Minneapolis, Minn. 61–72.

KNIGHT, B. W. 1972. Dynamics of encoding in a population of neurons. *J. Gen. Physiol.* **59:**734–766.

KNIGHT, B. W. 1973. Some questions concerning the encoding dynamics of neuron populations. Symposial papers, 4th International Biophysical Congress, Pushchino, Moscow. Academy of Sciences of the U. S. S. R. 422–436.

KNOX, C. K. 1970. Signal transmission in random spike trains with applications to the statocyst neurons of the lobster. *Kybernetik.* **7:**167–174.

MATTHEWS, P. B. C., and R. B. STEIN. 1969. The sensitivity of muscle spindle afferents to small sinusoidal changes in length. *J. Physiol. (Lond.).* **200:**723–743.

McKEAN, T. A., R. E. POPPELE, N. P. ROSENTHAL, and C. A. TERZUOLO. 1970. The biologically relevant parameter in nerve impulse trains. *Kybernetik.* **6:**168–170.

MICHAELIS, B., and R. A. CHAPLAIN. 1973. The encoder mechanism of receptor neurons. *Kybernetik.* **13:**6–23.

NELDER, J. A., and R. MEAD. 1964. A simplex method for function minimization. *Computer J.* **7**:308-313.

POPPELE, R. E. 1970*a*. The system approach to the function of the nervous system. Excitatory Synaptic Mechanisms. Universitetsforlaget, Oslo. 259-268.

POPPELE, R. E. 1970*b*. Encoder properties of muscle spindle receptors. *Fed. Proc.* **29**:522.

POPPELE, R. E., and R. J. BOWMAN. 1970. Quantitative description of linear behavior of mammalian muscle spindles. *J. Neurophysiol.* **33**:59-72.

POPPELE, R. E., and W. J. CHEN. 1972. Repetitive firing behavior of mammalian muscle spindle. *J. Neurophysiol.* **35**:357-364.

POPPELE, R. E., and R. L. PURPLE. 1971. Repetitive firing in receptor neurons. 25th International Congress of Physiological Science, Munich. 457.

PURPLE, R. L. 1970. Encoder properties of eccentric cells in the eye of *Limulus*. *Fed. Proc.* **29**:393.

PURPLE, R. L. and J. J. SALASIN. 1969. Negative feedback and pulse frequency modulation. *In* Systems Analysis in Neurophysiology. C. A. Terzuolo, editor. University of Minnesota, Minneapolis, Minn. 93-101.

RATLIFF, F., B. W. KNIGHT, and N. GRAHAM. 1969. Tuning and amplification by lateral inhibition. *Proc. Natl. Acad. Sci. U. S. A.* **62**:733-740.

RESCIGNO, A., R. B. STEIN, R. L. PURPLE, and R. E. POPPELE. 1970. A neuronal model for the discharge patterns produced by cyclic inputs. *Bull. Math. Biophys.* **32**:337-353.

SOKOLOVE, P. G., and J. M. COOKE. 1971. Inhibition of impulse activity in a sensory neuron by an electrogenic pump. *J. Gen. Physiol.* **57**:125-163.

STEIN, R. B. 1970. The role of spike trains in distorting and transmitting sensory signals. *In* The Neurosciences. Vol. II. The Rockefeller University Press, New York. 597.

STEIN, R. B., and A. S. FRENCH. 1970. Models for the transmission of information by nerve cells. *In* Excitatory Synaptic Mechanisms. Universitetsforlaget, Oslo. 247-257.

STEVENS, C. E. 1964. A. quantitative theory of neural interactions: Theoretical and experimental investigations. Ph.D. Thesis. The Rockefeller University, New York.

TERZUOLO, C. A., and Y. WASHIZU. 1962. Relation between stimulus strength, generator potential and impulse frequency in stretch receptor of crustacea. *J. Neurophysiol.* **25**:56-66.